Introduction to Synthetic Aperture Radar (SAR) and SAR-Interferometry (InSAR)

Konstantinos P. Papathanassiou

German Aerospace Center (DLR)
Microwaves and Radar Institute (DLR-HR)
Pol-InSAR Research Group

Oberpfaffenhofen, P.O. 1116, D-82234 Wessling
Tel./Fax.: ++49-(0)8153-28-2367/1149
Email: kostas.papathanassiou@dlr.de

Electromagnetic Spectrum & Remote Sensing Techniques

Passive: Microwave Radiometer TIR Imager VNIR Imager

Active: Radar Imager & Altimeter Profiler Laser Profilers

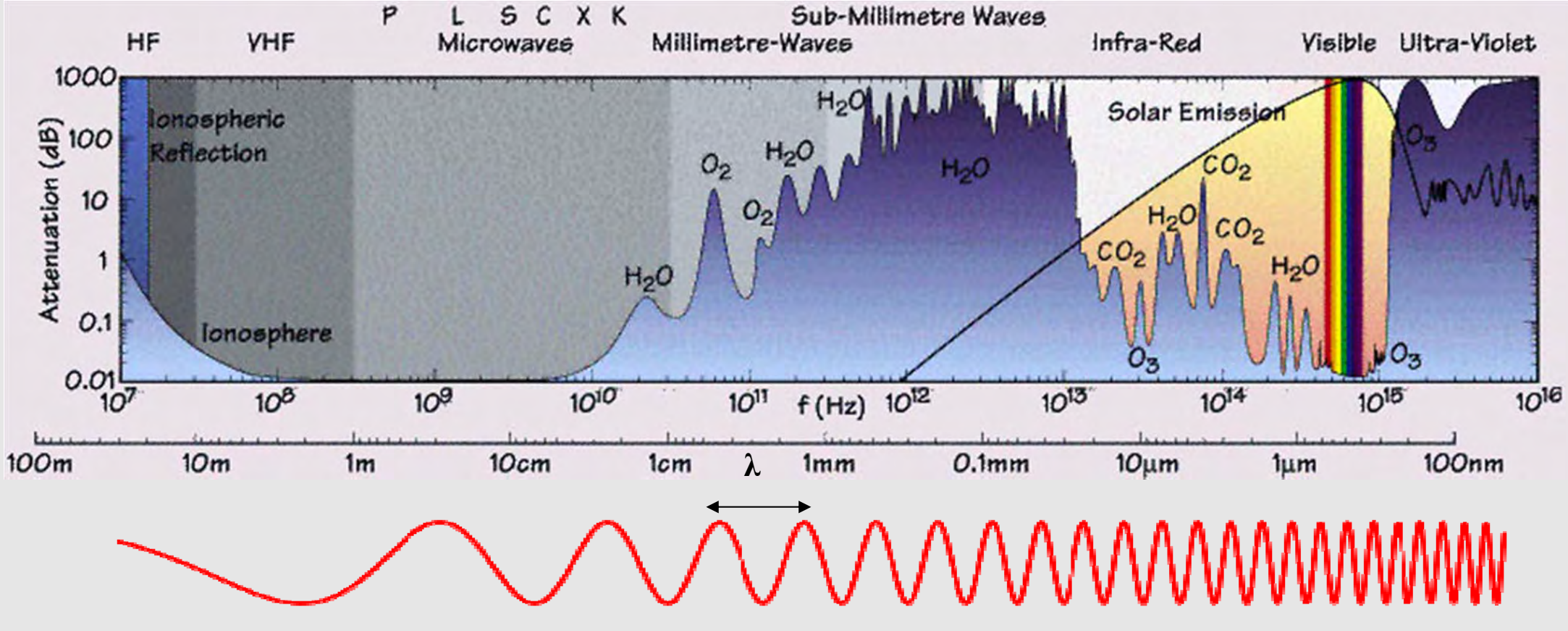

Electromagnetic spectrum and attenuation caused by Earth's atmosphere

Unique Characteristics of Microwave Remote Sensing

- **Independent of Weather Conditions: Penetrate clouds, rain, (smoke);**

- (Lower Frequencies) Penetrate into / through a wide class of natural cover types as: Sand / Ice / Vegetation;

- Sensitive to objects of dimensions from cm to m: (Complementary to Optical and IR remote sensing);

- Very accurate (differential) distance measurements (employing interferometric techniques);

- (Active) Microwave systems are able to operate day and night.

Global Annual Mean Cloud Cover (2007-2009)

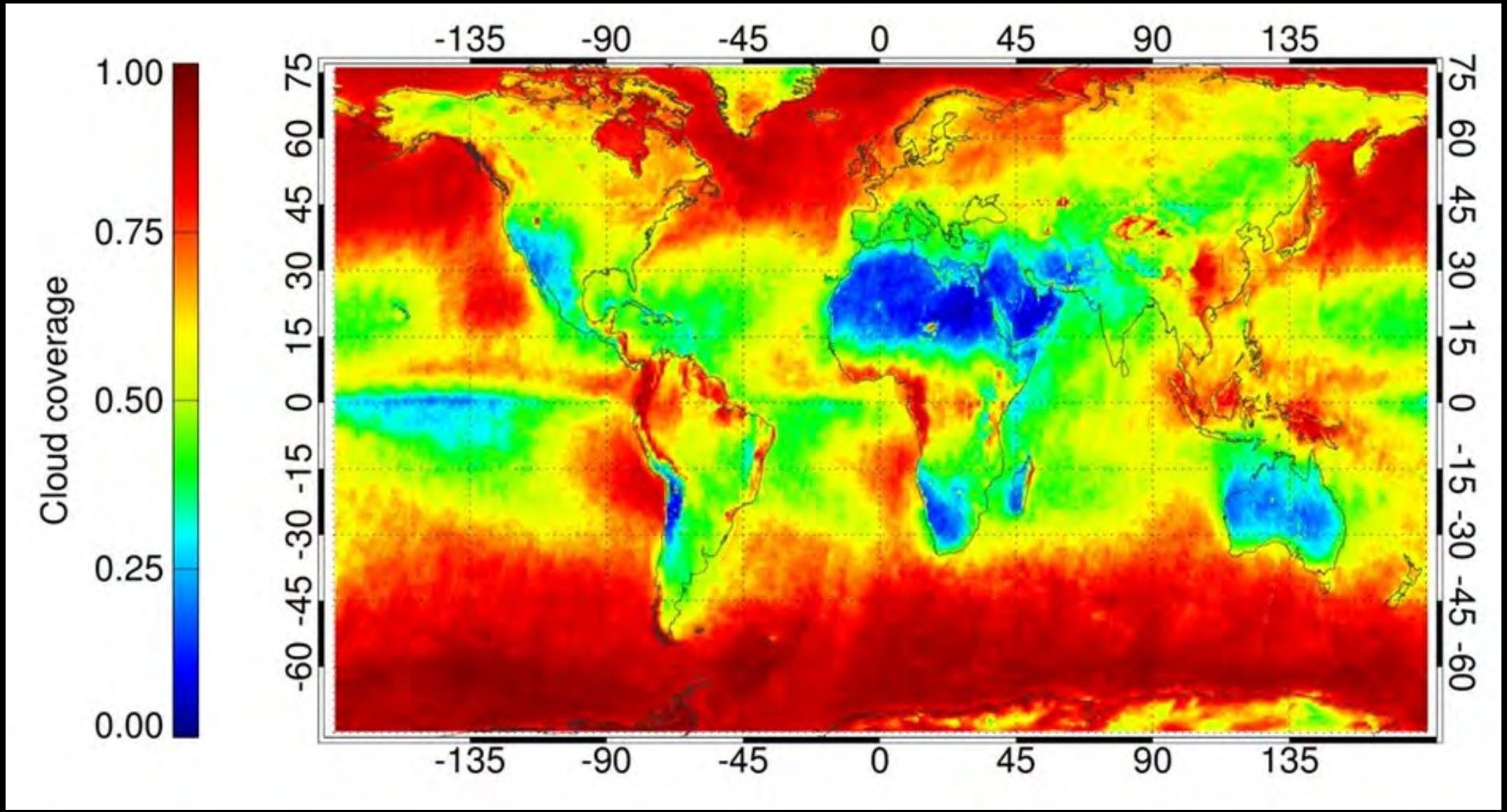

From MERIS and AATSR on ENVISAT

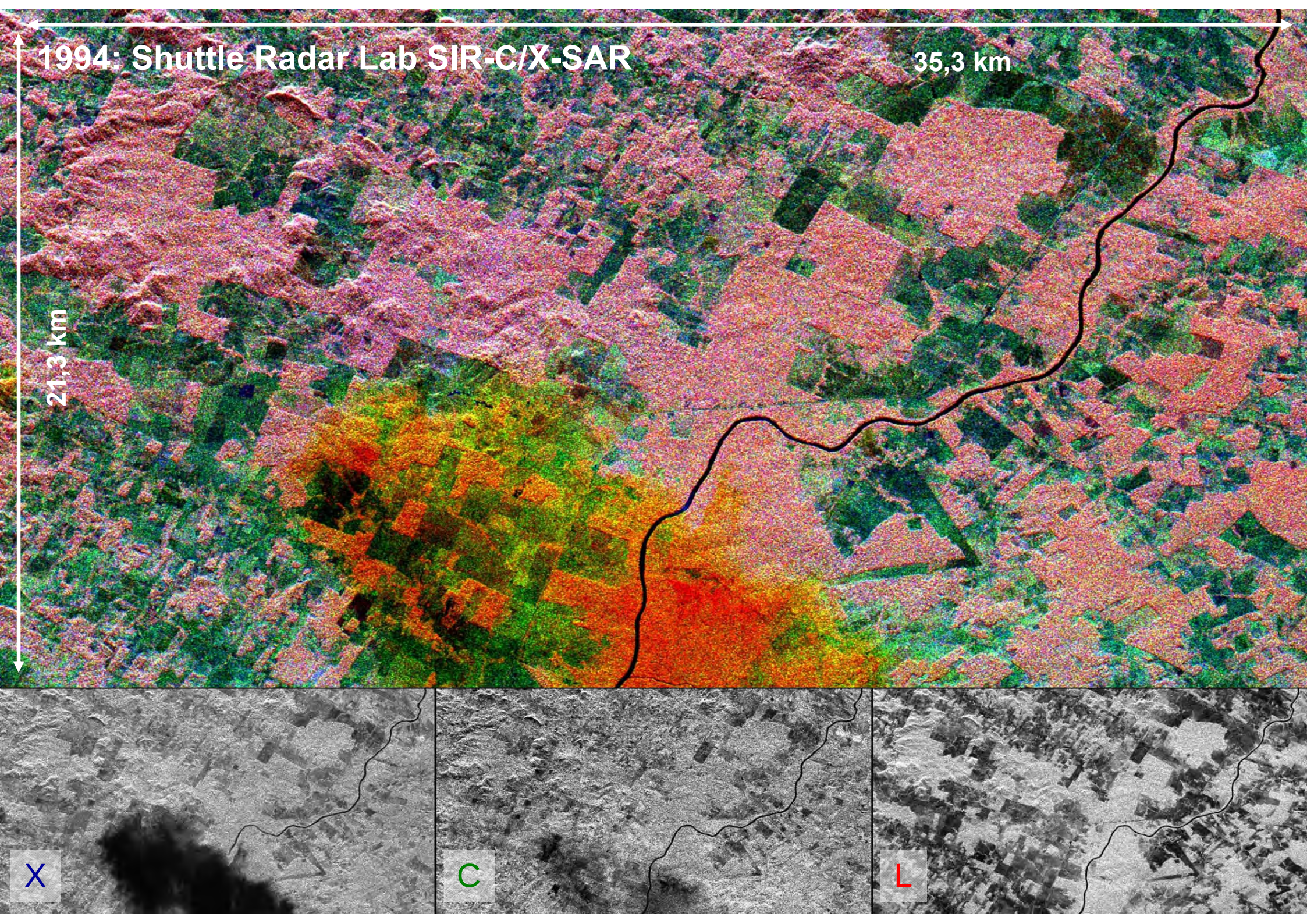
1994: Shuttle Radar Lab SIR-C/X-SAR
35,3 km
21,3 km
X
C
L

Unique Characteristics of Microwave Remote Sensing

- Independent of Weather Conditions: Penetrate clouds, rain, (smoke);

- **(Lower Frequencies) Penetrate into / through a wide class of natural cover types as: Sand / Ice / Vegetation;**

- Sensitive to objects of dimensions from cm to m: (Complementary to Optical and IR remote sensing);

- Very accurate (differential) distance measurements (employing interferometric techniques);

- (Active) Microwave systems are able to operate day and night.

Penetration into Vegetation

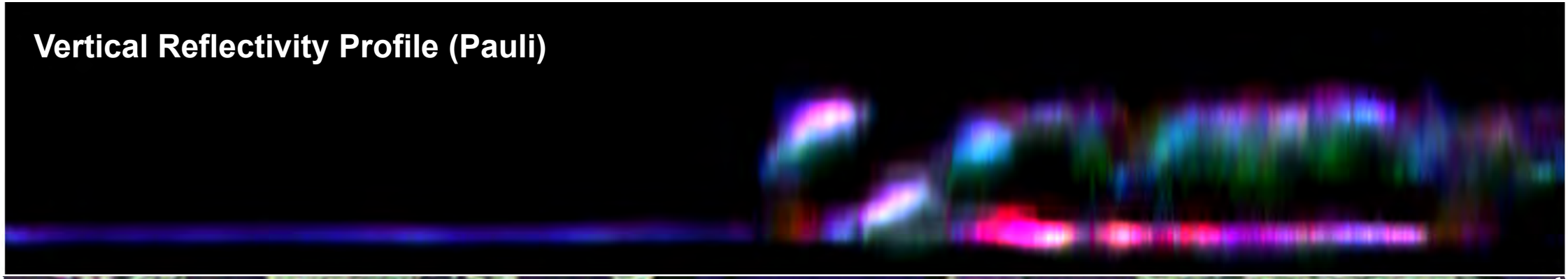

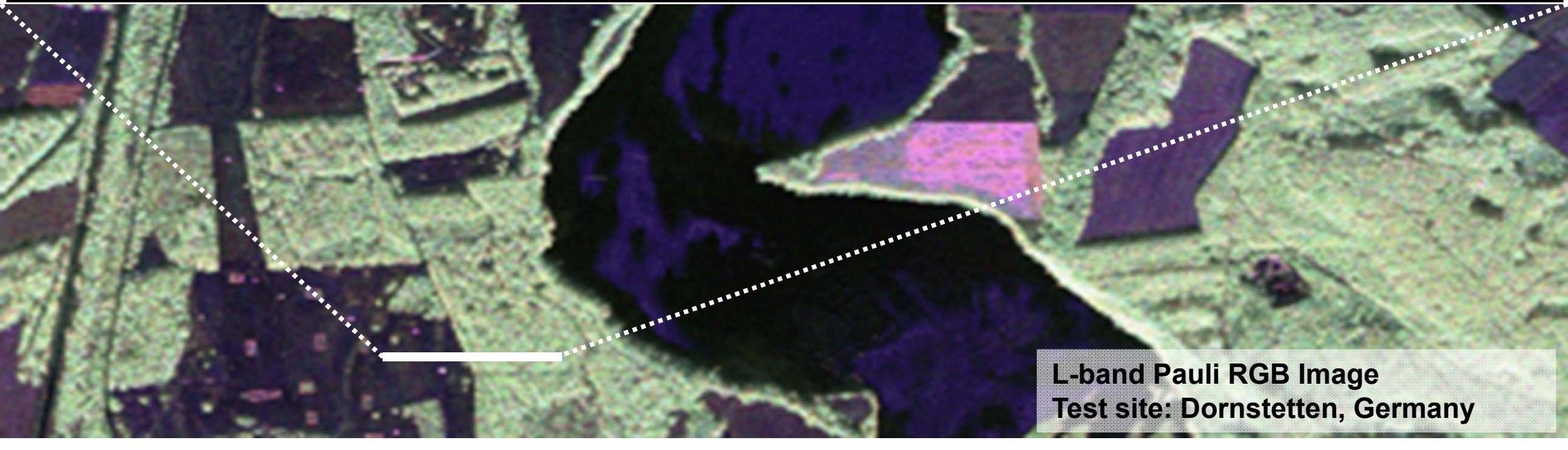

Penetration into Ice

Surface

~300m

Bedrock

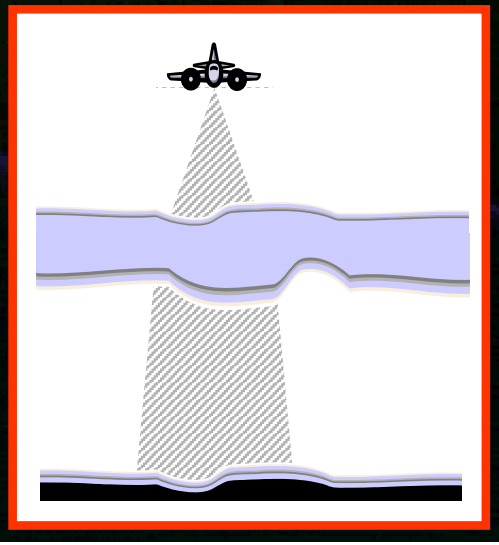

E-SAR / Test Site: Glacier Austfonna, Svalbard

Frequency Range & Penetration into / through Natural Media

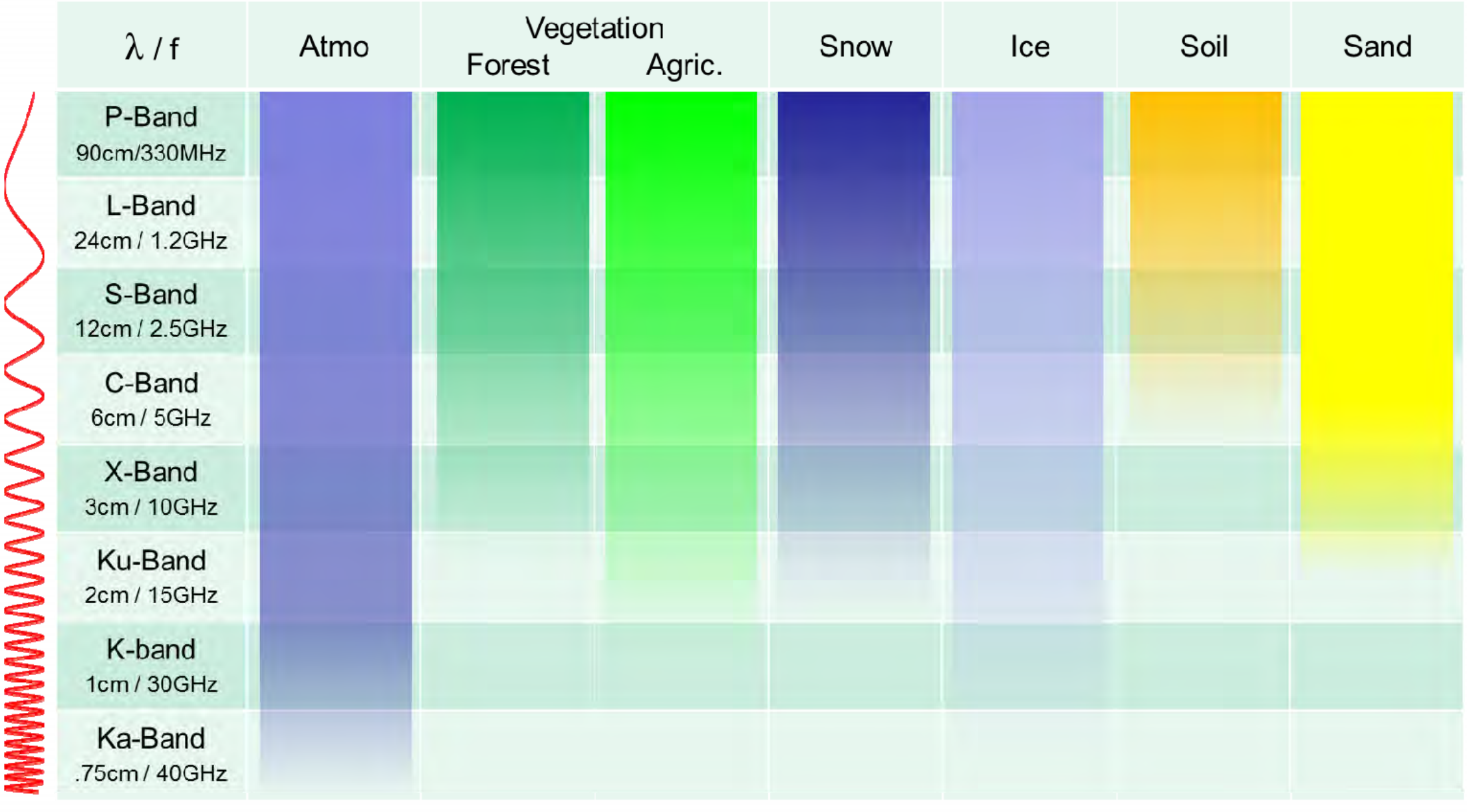

Unique Characteristics of Microwave Remote Sensing

- Independent of Weather Conditions: Penetrate clouds, rain, (smoke);
- (Lower Frequencies) Penetrate into / through a wide class of natural cover types as: Sand / Ice / Vegetation;
- **Sensitive to objects of dimensions from cm to m: (Complementary to Optical and IR remote sensing);**
- Very accurate (differential) distance measurements (employing interferometric techniques);
- (Active) Microwave systems are able to operate day and night.

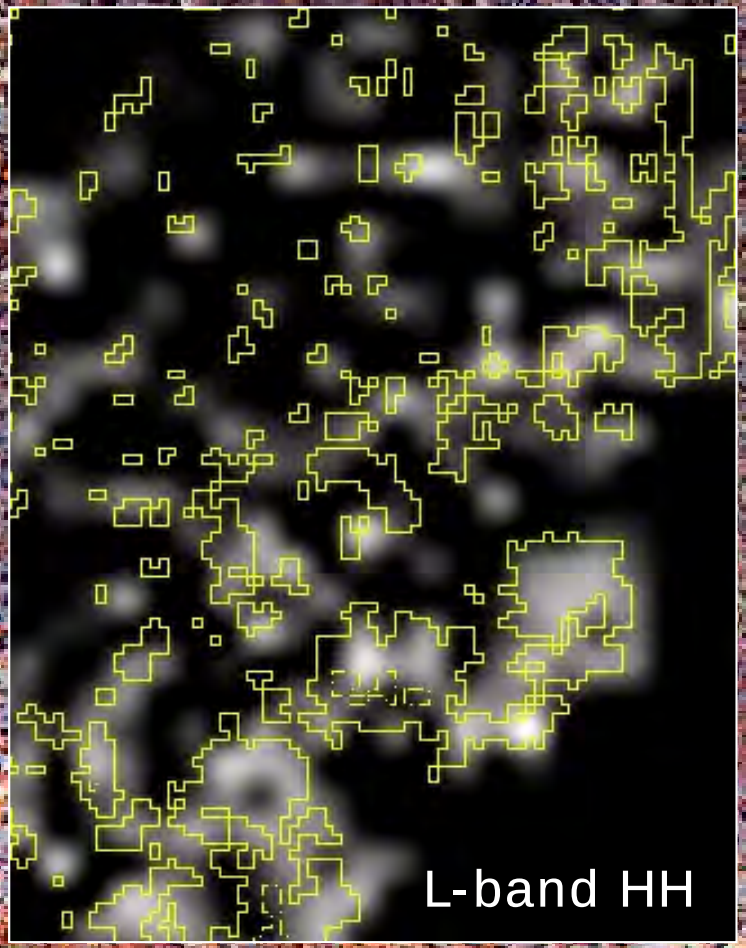

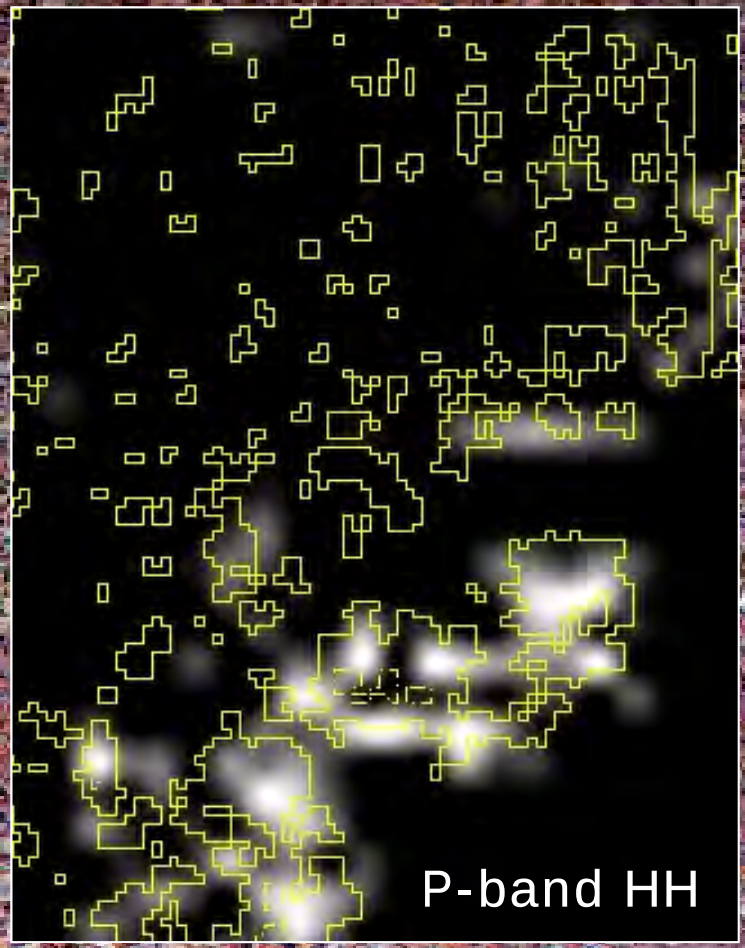

Injune, QL, Australia

Prifysgol Cymru Aberystwyth
1872 The University of Wales

Unique Characteristics of Microwave Remote Sensing

- Independent of Weather Conditions: Penetrate clouds, rain, (smoke);
- (Lower Frequencies) Penetrate into / through a wide class of natural cover types as: Sand / Ice / Vegetation;
- Sensitive to objects of dimensions from cm to m: (Complementary to Optical and IR remote sensing);
- **Very accurate (differential) distance measurements (employing interferometric techniques);**
- (Active) Microwave systems are able to operate day and night.

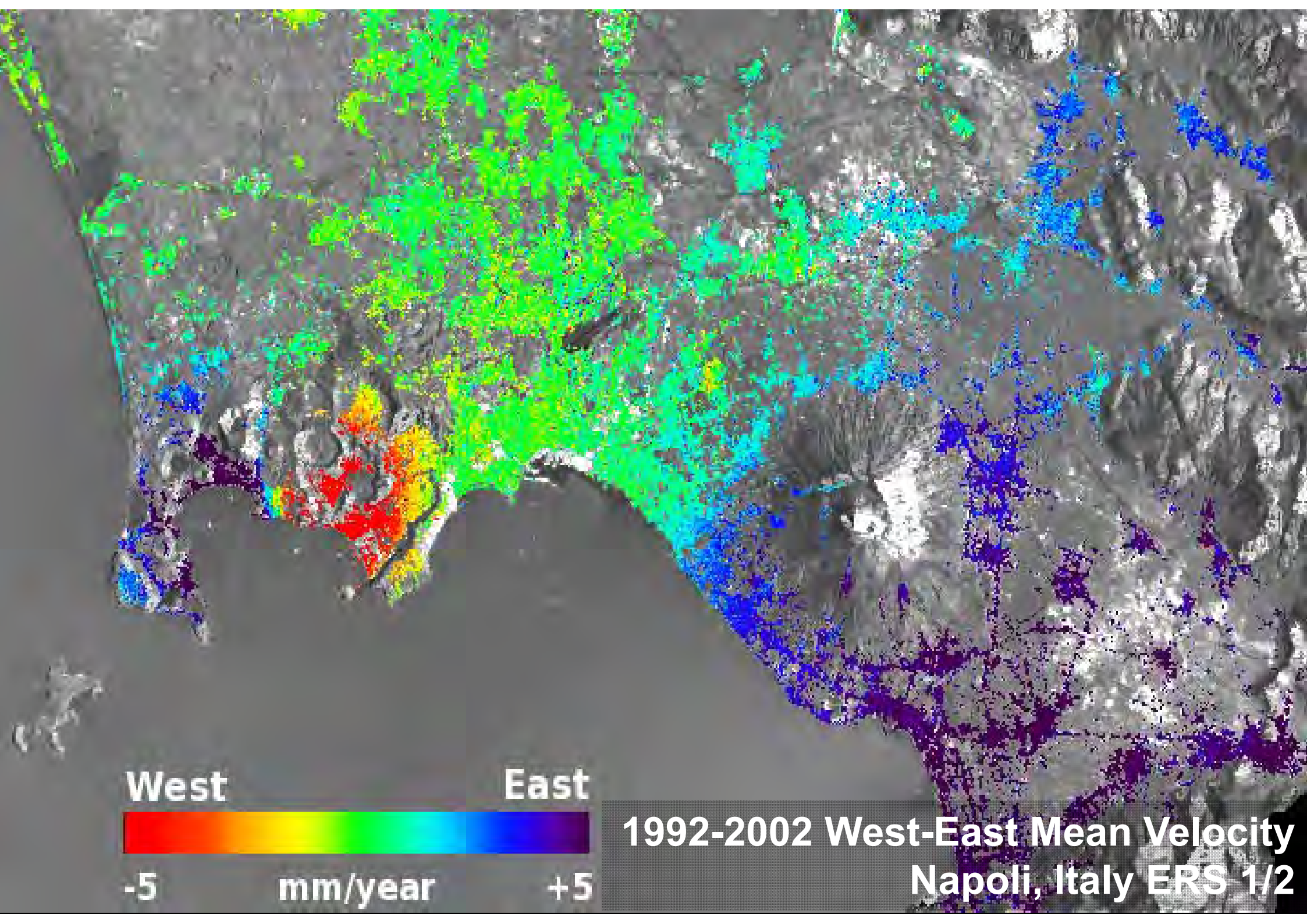
West
East
-5
mm/year
+5
1992-2002 West-East Mean Velocity
Napoli, Italy ERS 1/2

Unique Characteristics of Microwave Remote Sensing

- Independent of Weather Conditions: Penetrate clouds, rain, (smoke);
- (Lower Frequencies) Penetrate into / through a wide class of natural cover types as: Sand / Ice / Vegetation;
- Sensitive to objects of dimensions from cm to m: (Complementary to Optical and IR remote sensing);
- Very accurate (differential) distance measurements (employing interferometric techniques);
- **(Active) Microwave systems are able to operate day and night.**

© ESA ENVISAT
30-5-2008

In the Wilkins Ice Shelf an area of about 160 km² collapsed during the Antarctic winter 2008.

This animation, comprised of images acquired by Envisat's Advanced Synthetic Aperture Radar (ASAR) between 30 May and 9 June 2008, highlights the rapidly windling strip of ice that is protecting thousands of kilometres of the ice shelf from further break-up.

This was the first ever-documented episode to occur in winter.

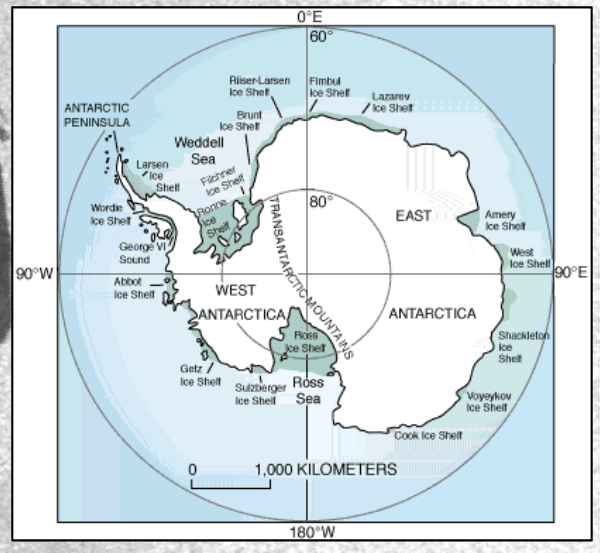

SAR Remote Sensing and Global Societal Challenges

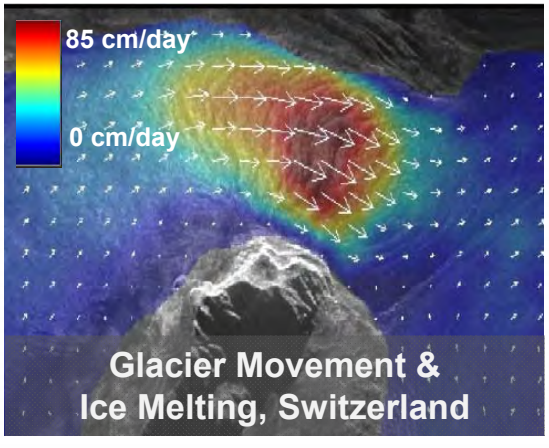

Climate Change

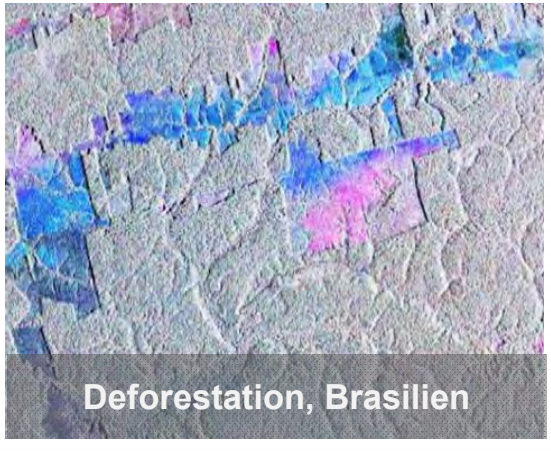

Environment

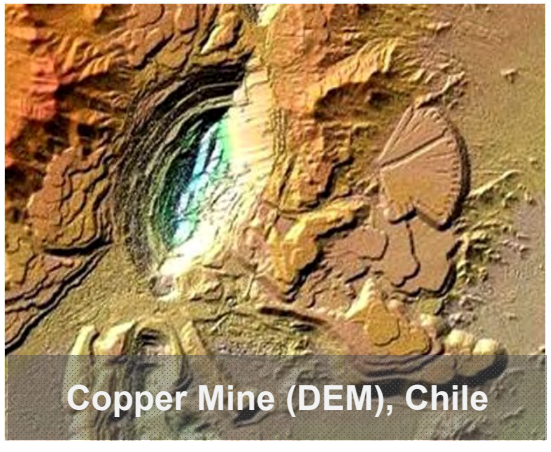

Resources

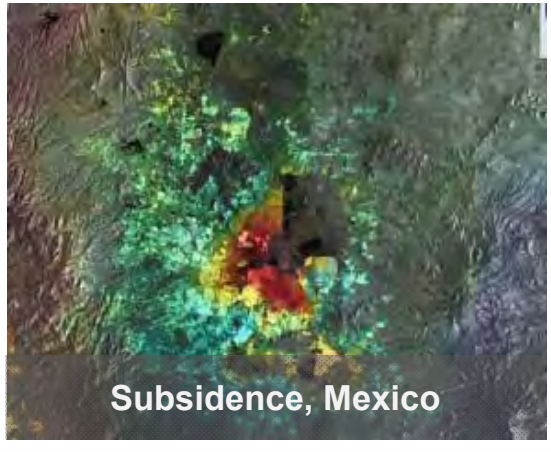

Sustainable Development

Megacities

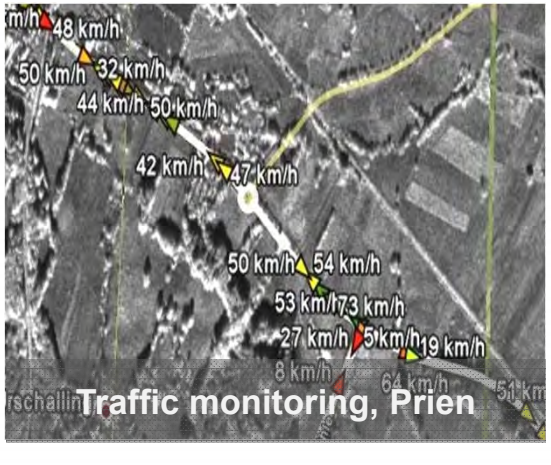

Mobility

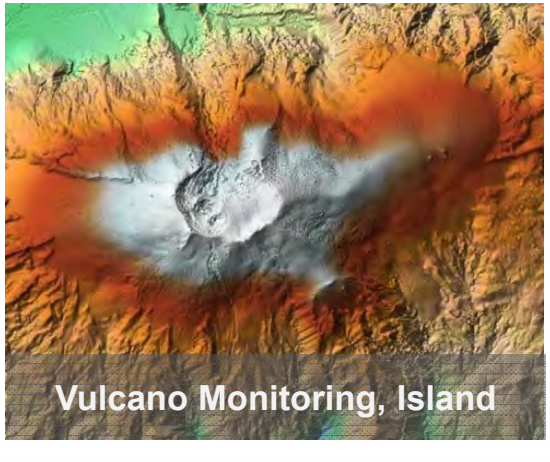

Hazards

Disaster

DLR Deutsches Zentrum für Luft- und Raumfahrt e.V.
in der Helmholtz-Gemeinschaft

Basic Radar Operation Block Diagram

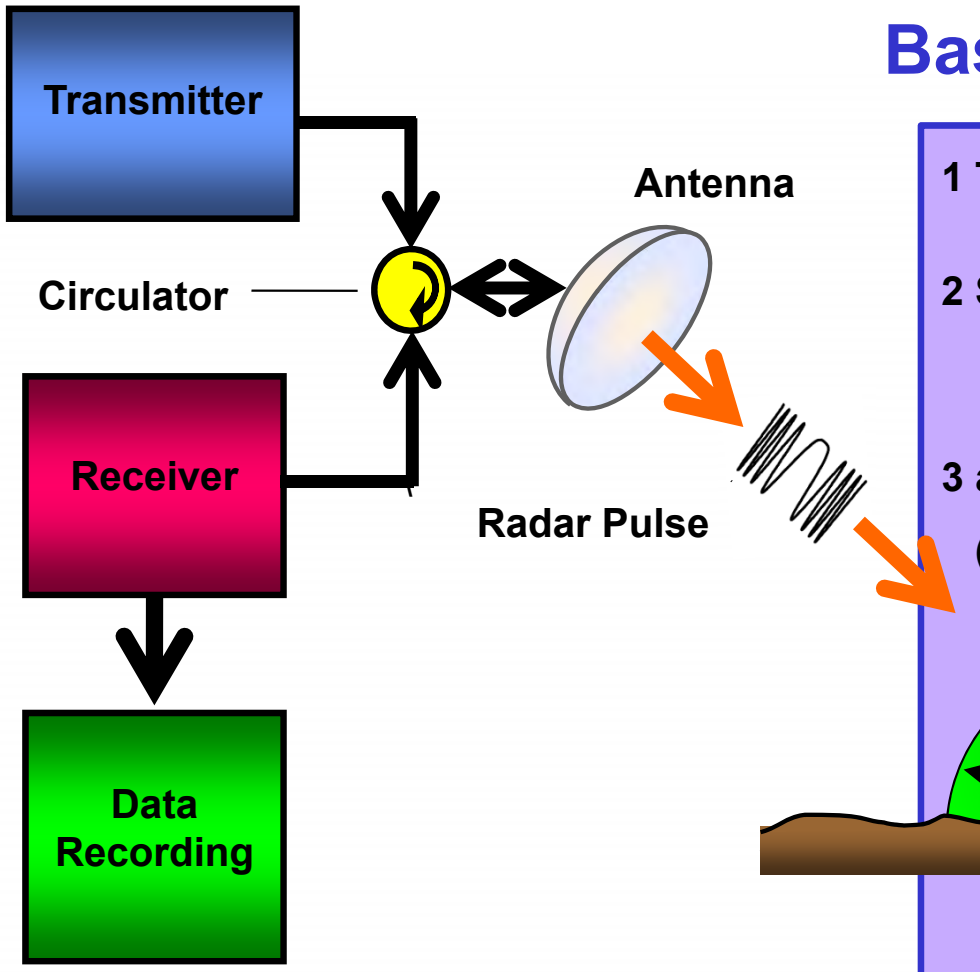

1 The transmitted pulse interacts with the scene / scatterer;

2 Some of the energy of the incident radar pulse is scattered back towards the radar

3 and is measured by the radar. It is known as the scatterer's (complex) radar reflectivity (radar brightness).

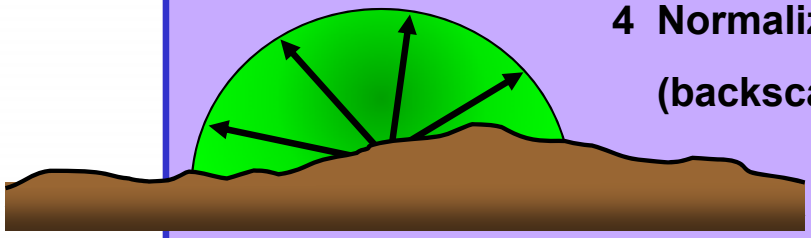

4 Normalized radar cross-section (backscattering coefficient):

$$\sigma_o\,[dB] = 10.\log_{10}\left(\frac{E}{E_{iso}}\right)$$

E: Energy received from (backscattered by) the scatterer

E_{iso}: Energy received from (backscattered by) an isotropic scatterer

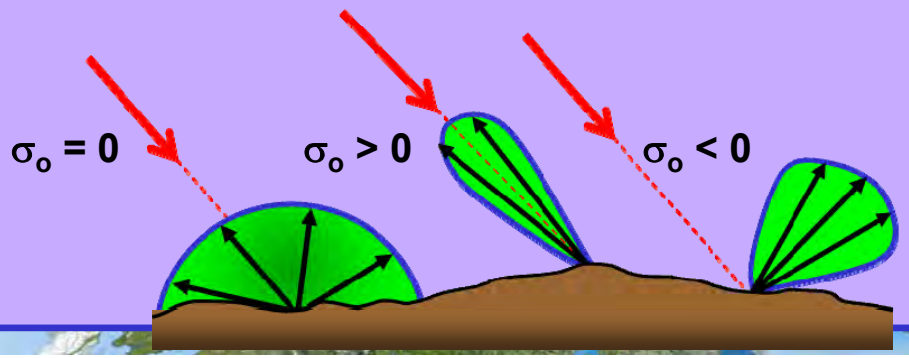

- **Transmitter: generates a high power pulse;**
- **Circulator** (Switch)**: switches the transmitted pulse to the antenna, & the returned echoes to the receiver;**
- **Antenna directs the transmitted pulse towards the scene;**
- **Receiver amplifies the received signal and converts to base band.**

Side-Looking Imaging Geometry

Pulsed radar system

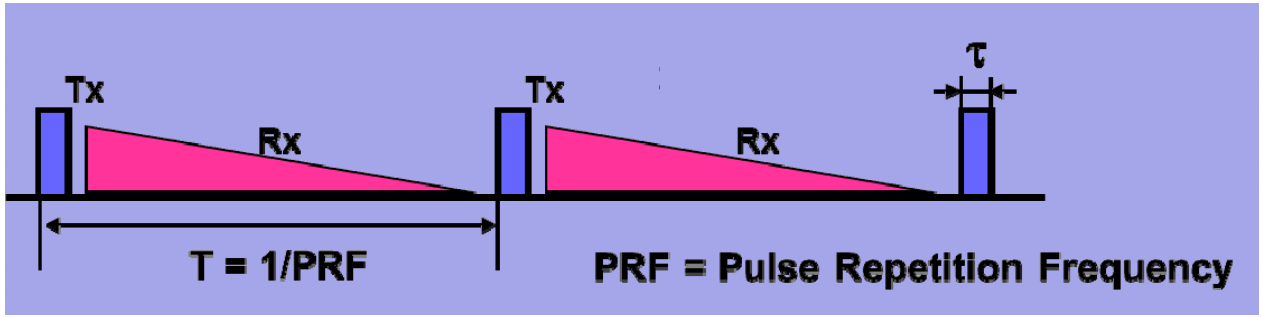

2-D Imaging: Azimuth x (Slant) Range

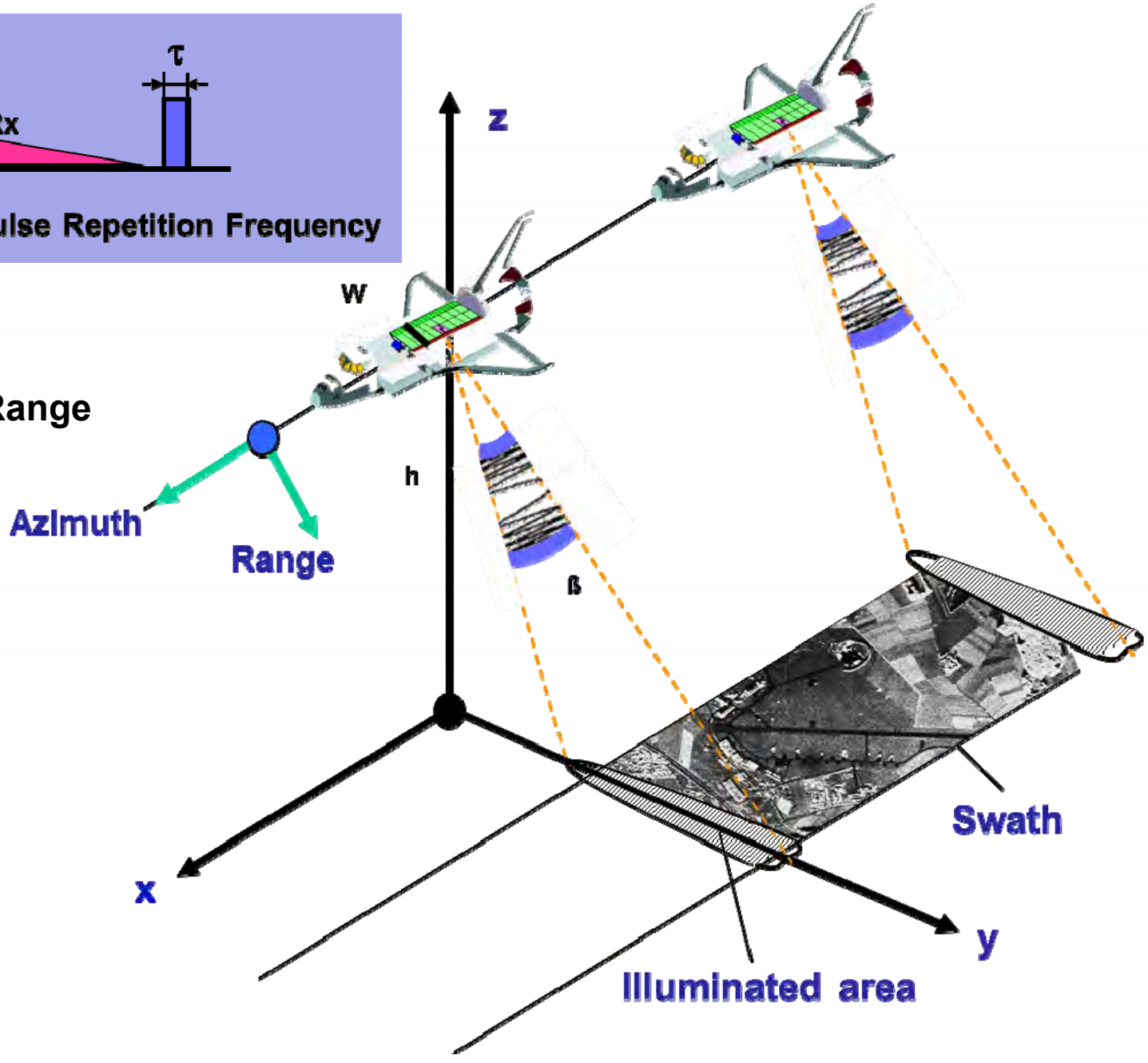


Amazon Deforest Watch (Santarem) ALOS PalSAR
2007/6/13
2007/9/13
80Km
Lat : S 2°34'
Lon : W 54°45'

Drygalski Glacier Oct 2007 – Jul 2008

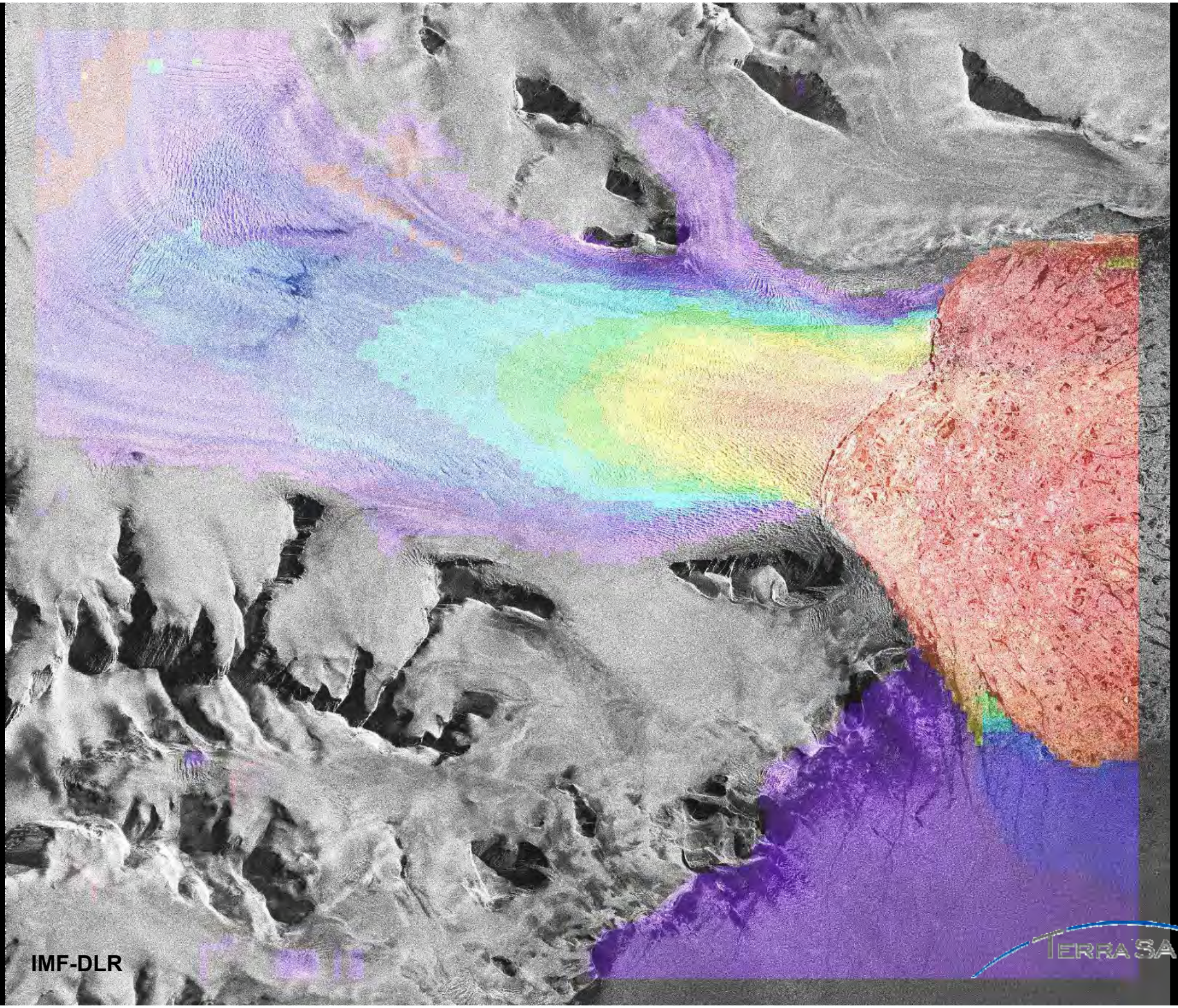

DLR

IMF-DLR

TERRASAR X

SAR Interferometry (InSAR)

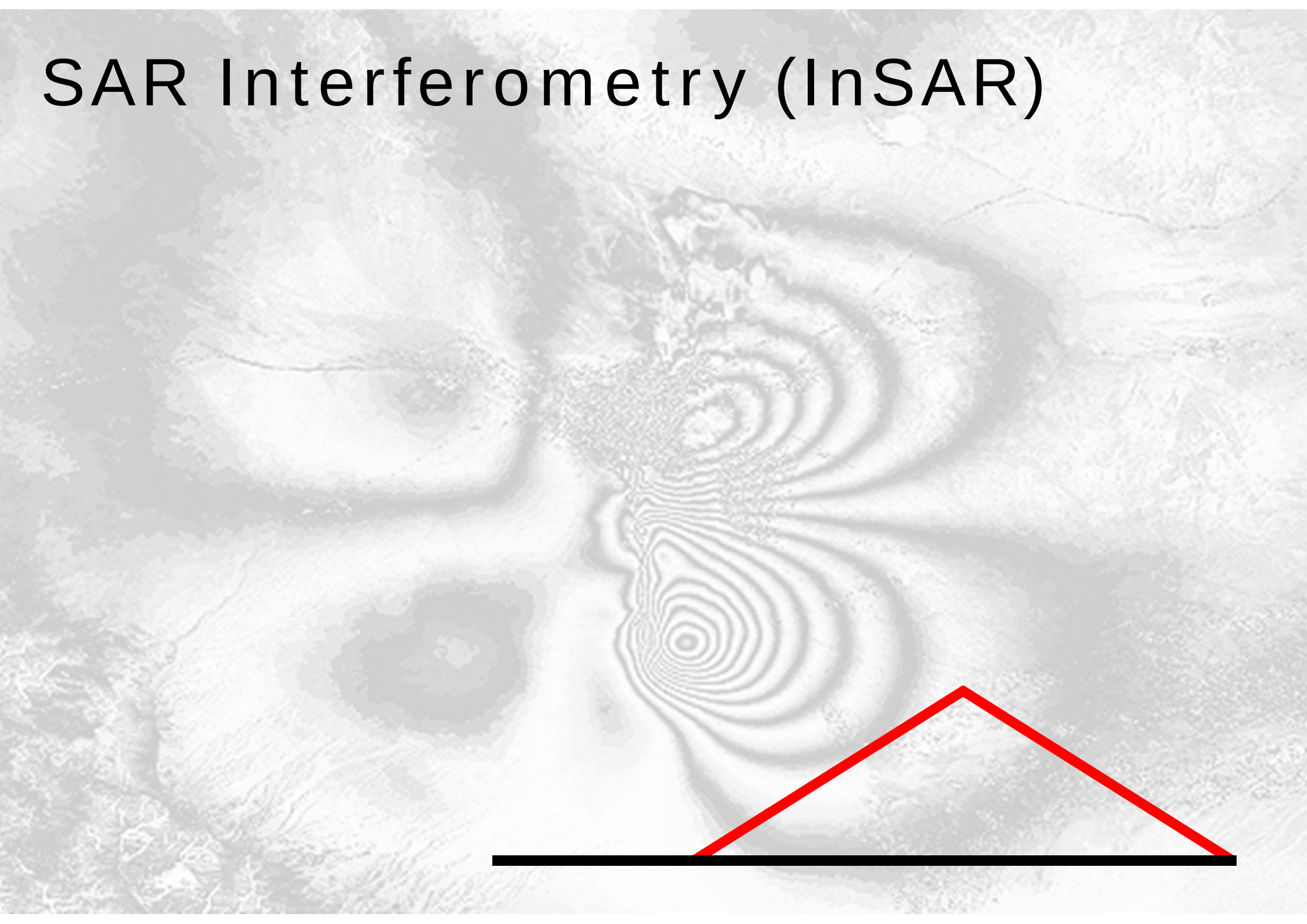

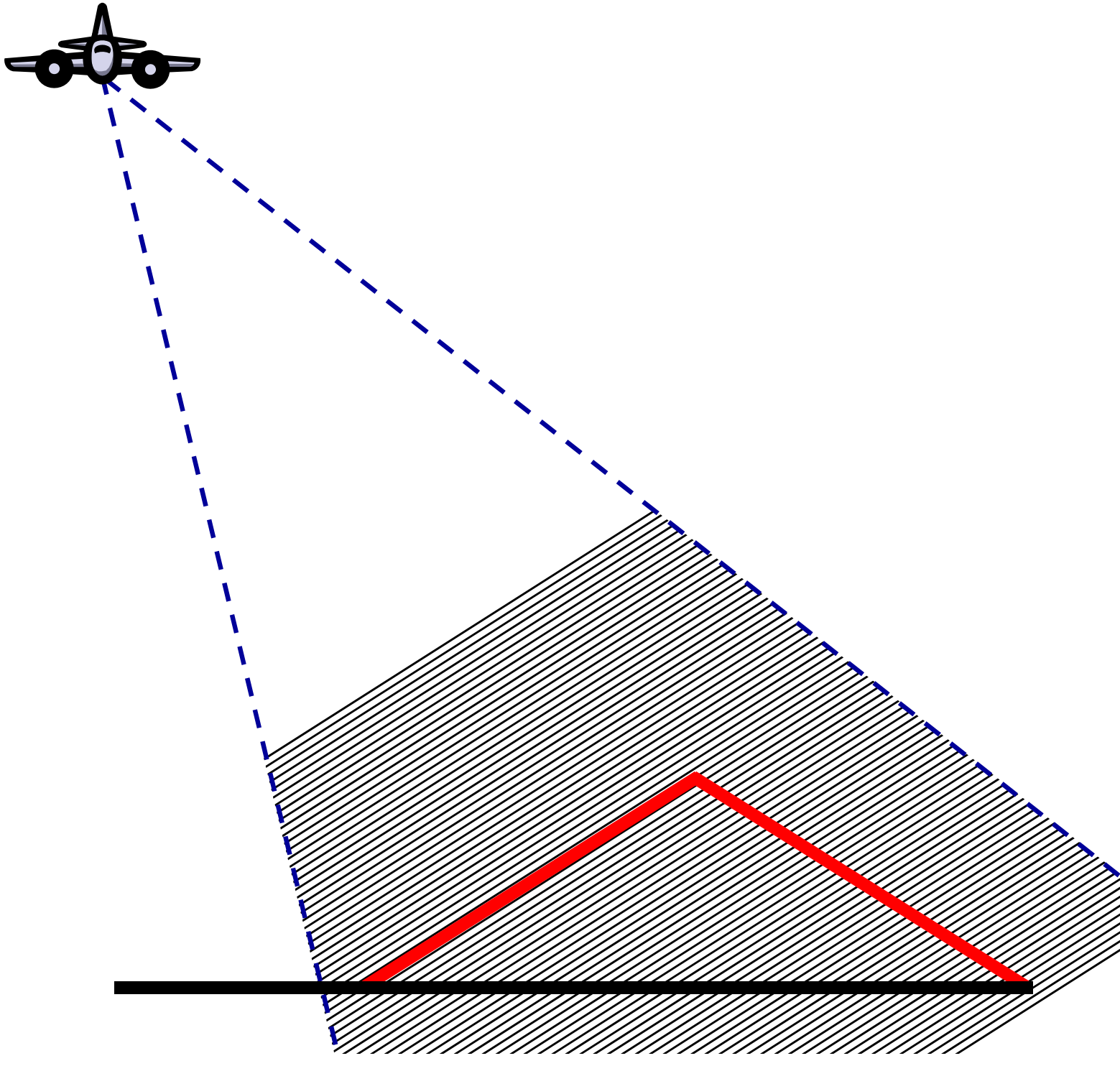

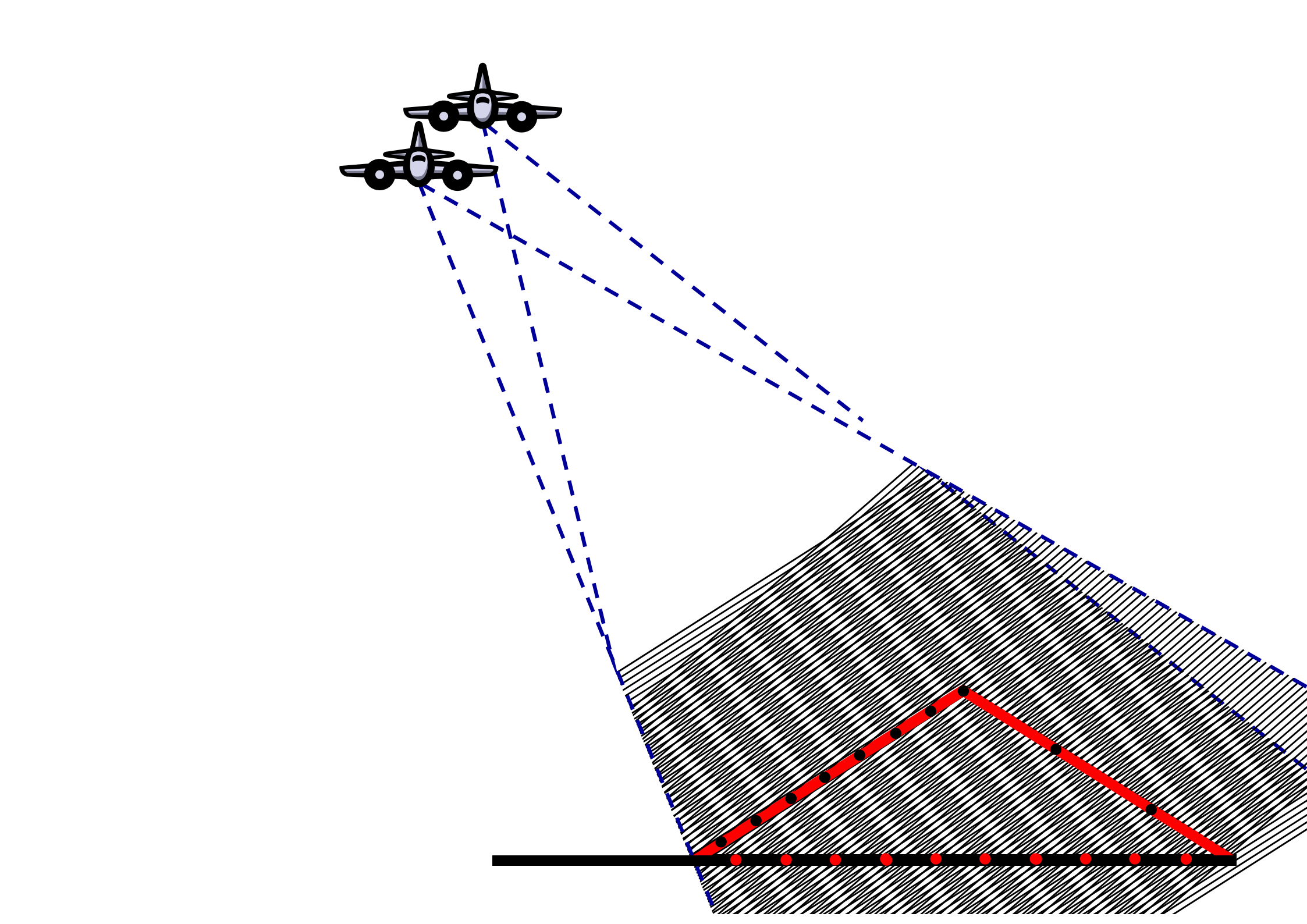

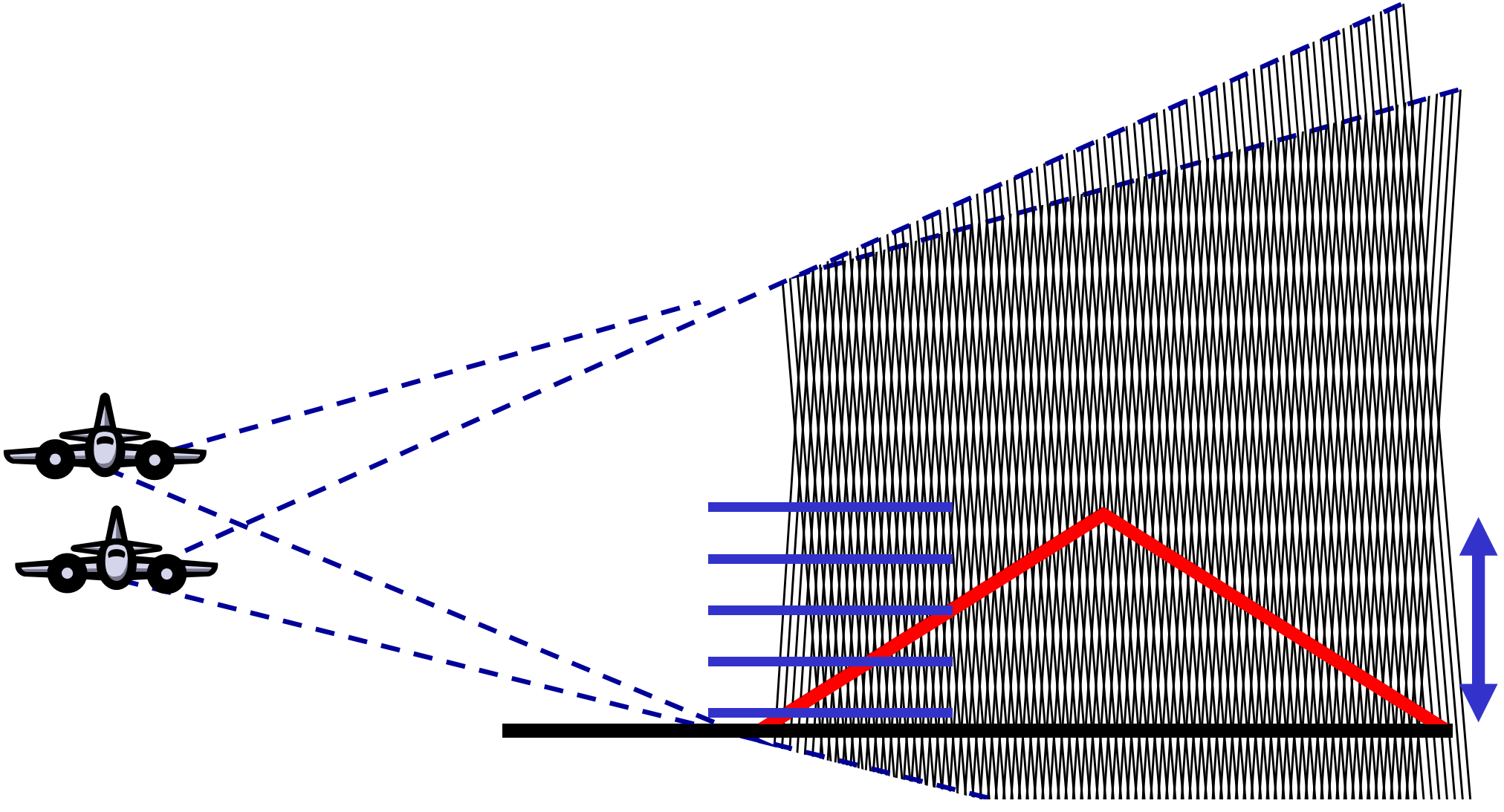

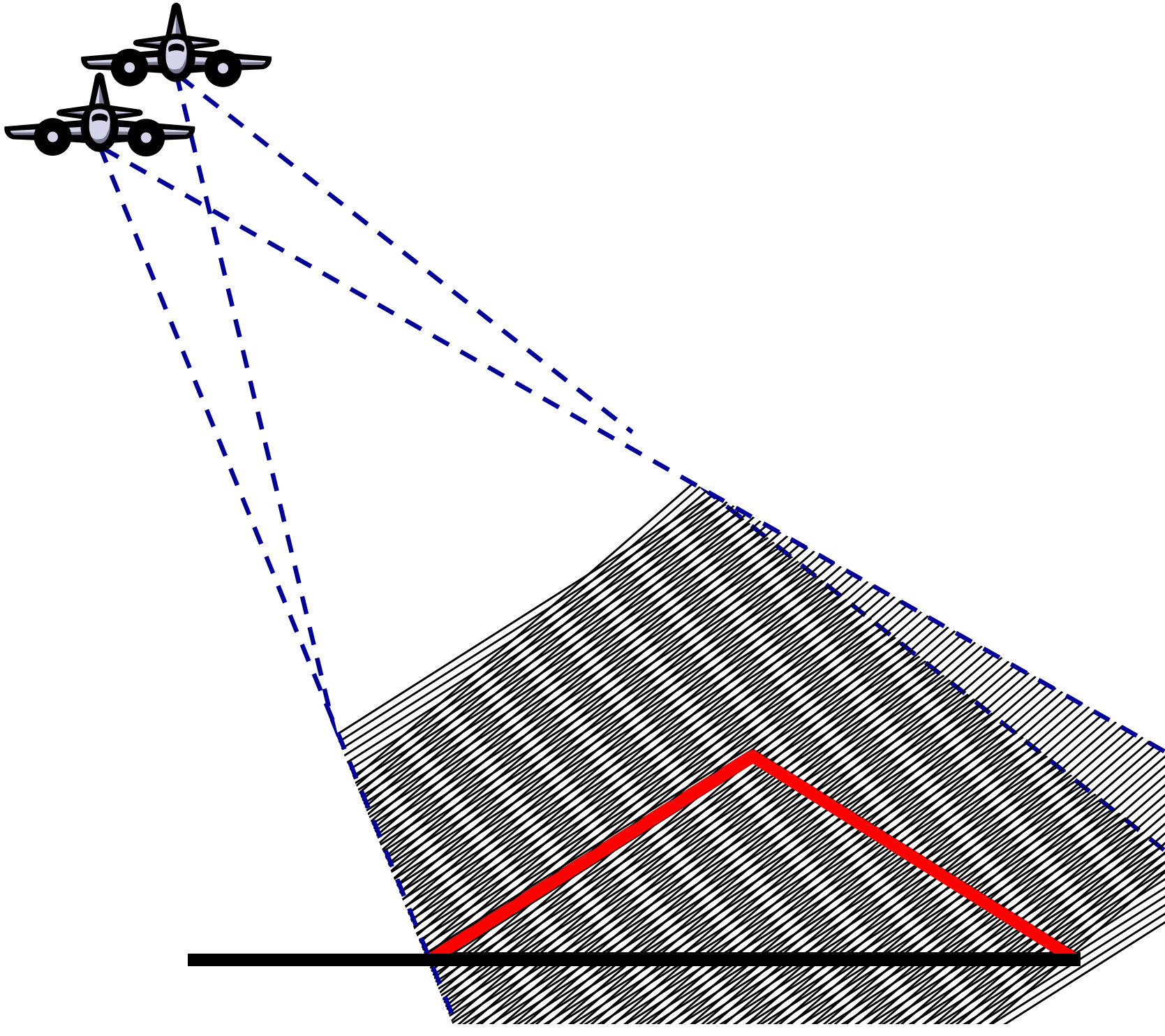

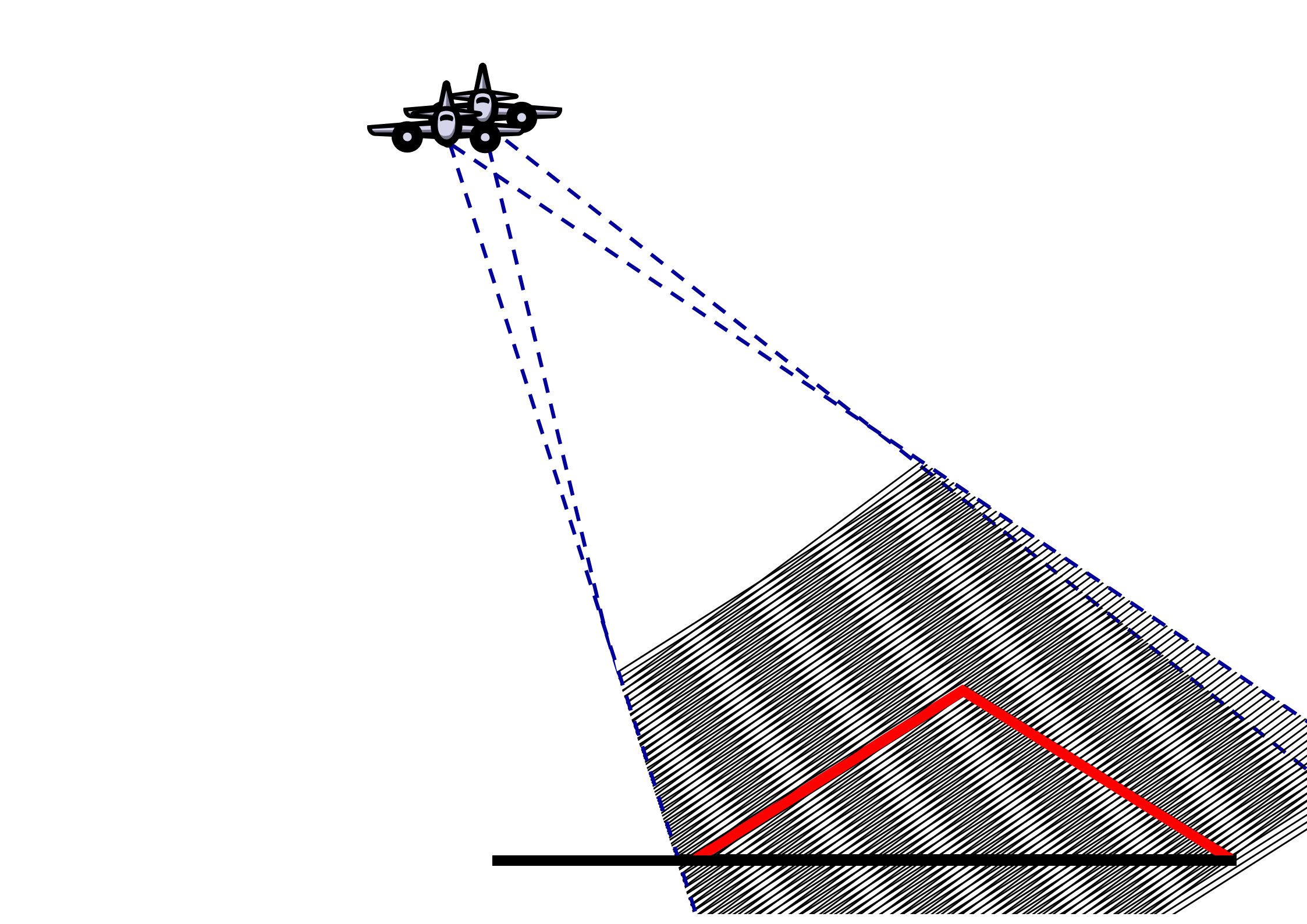

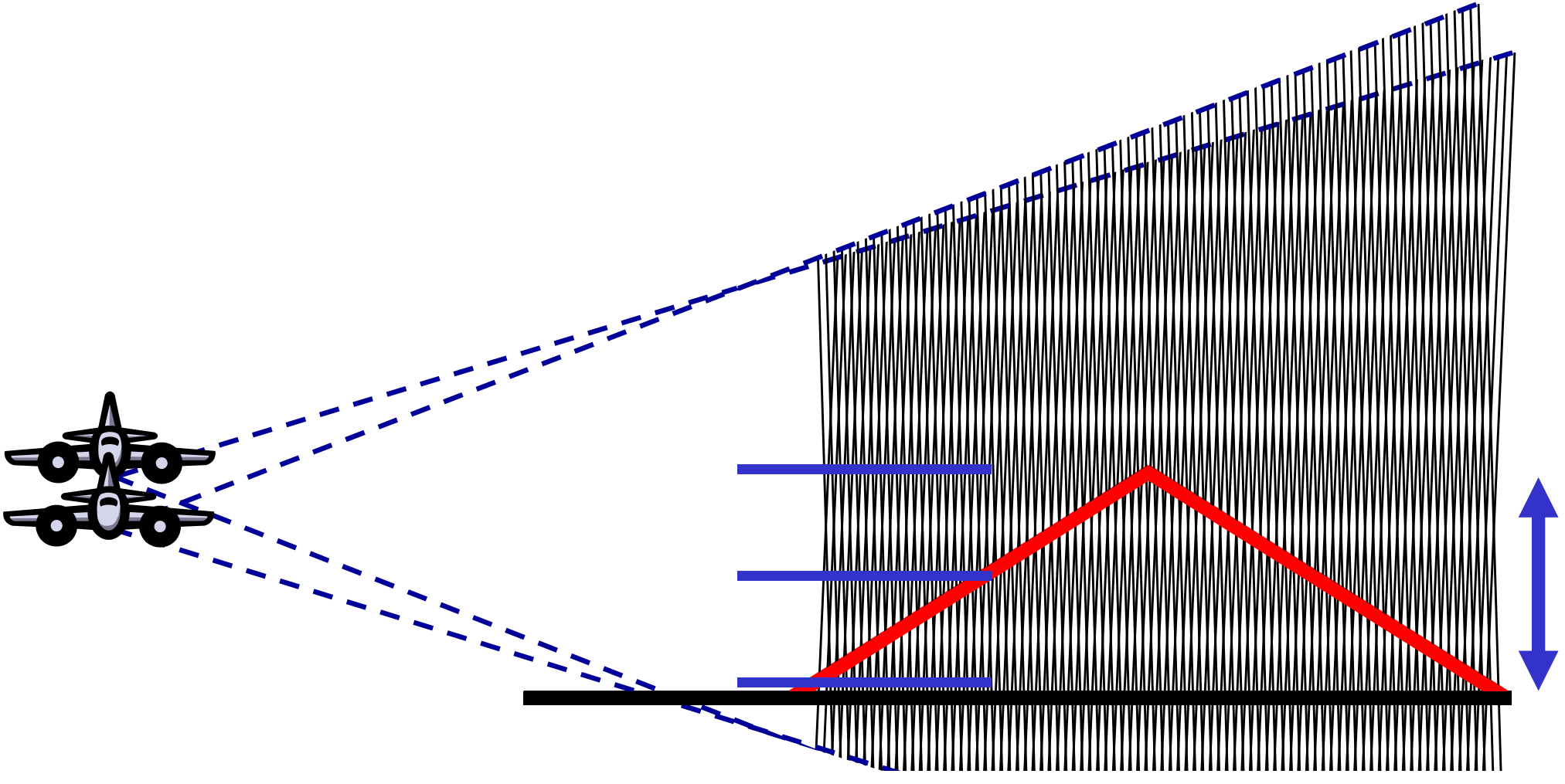

The Phase-to-Height Sensitivity increases with increasing the spatial baseline (i.e. $\Delta\theta$ or $B_{\perp}$);

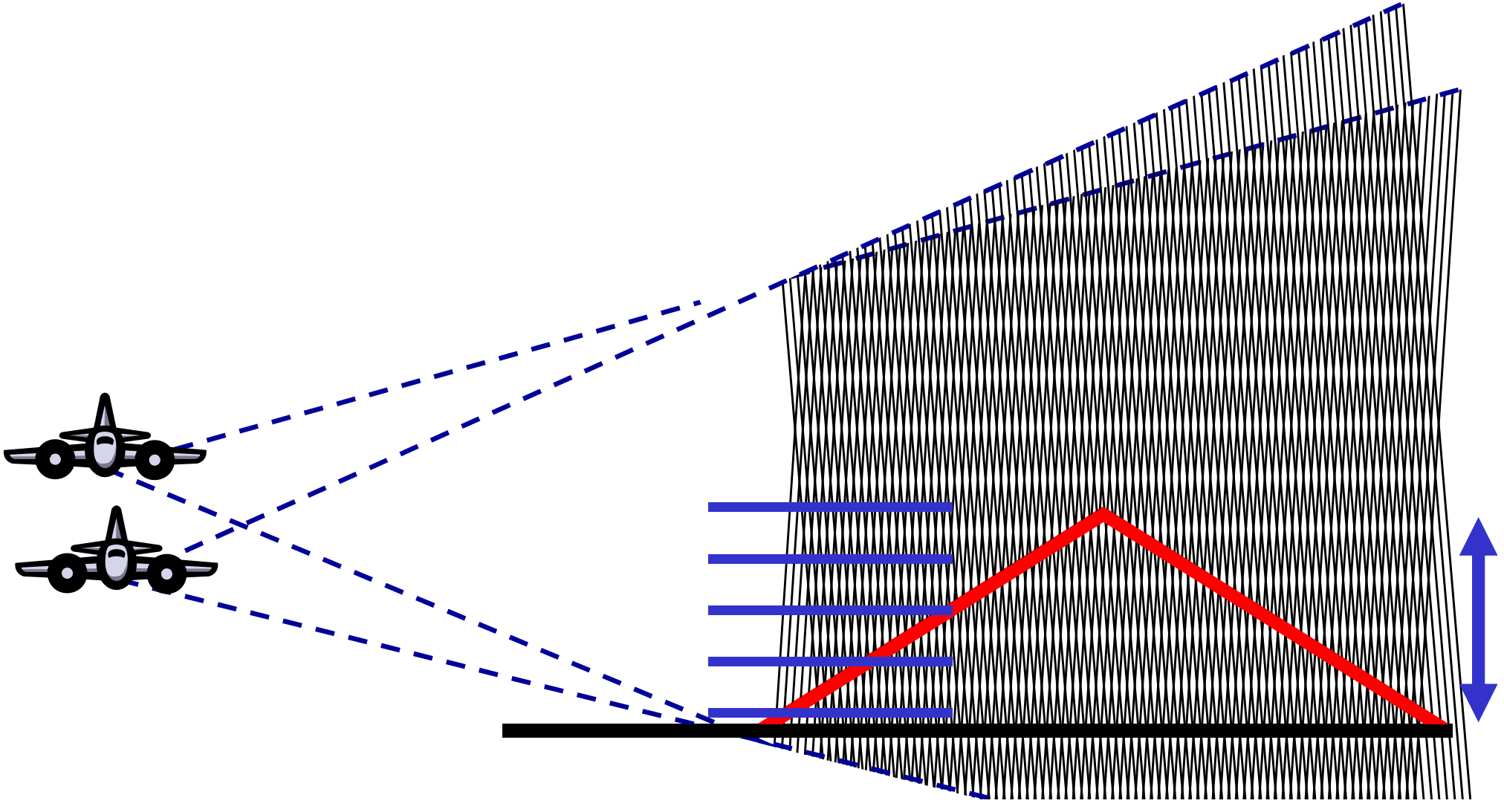

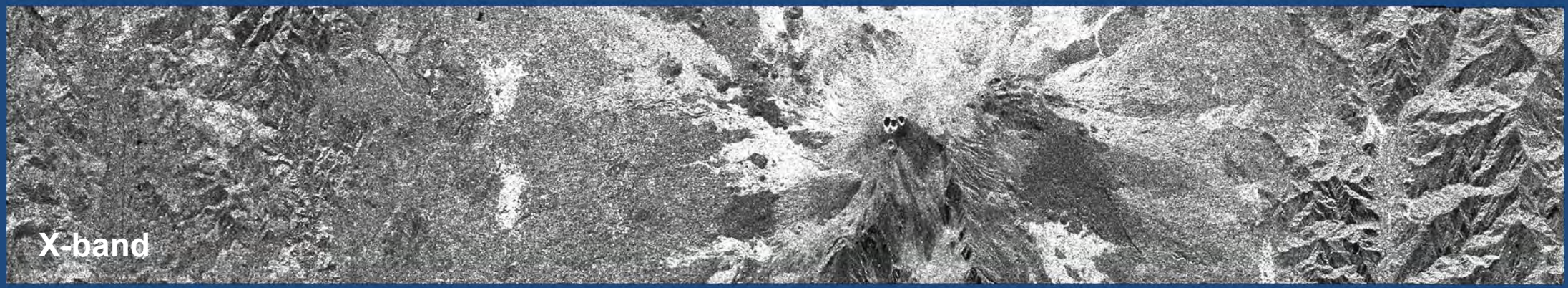

Amplitude Images

24 Hours Temporal Baseline

SIR-C / Test Site: Mt. Etna, Italy

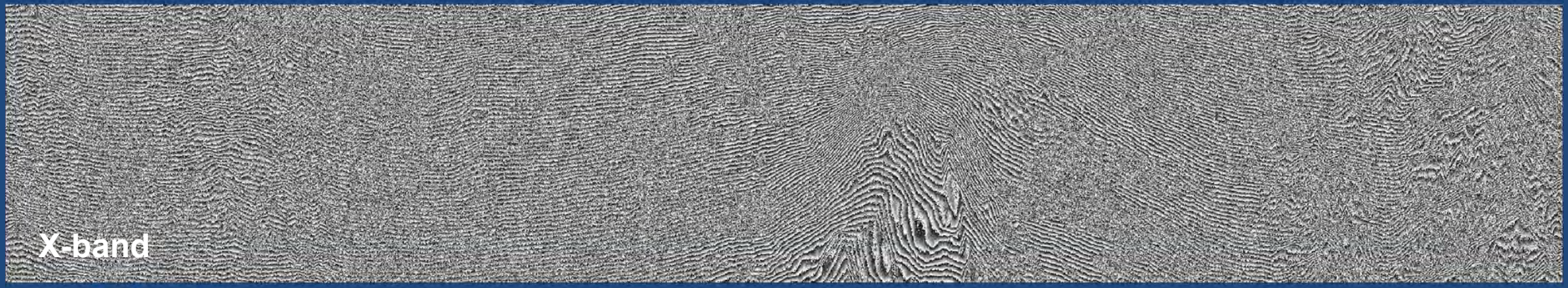

Phase Images

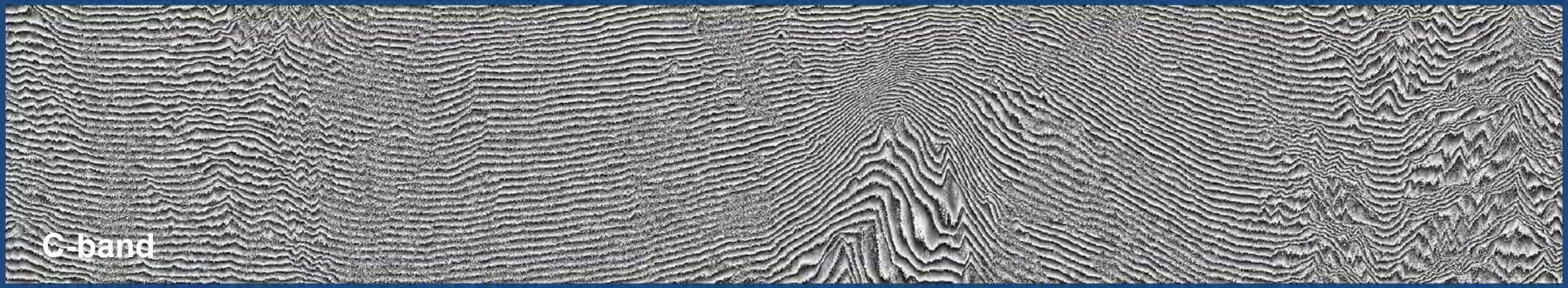

SIR-C / Test Site: Mt. Etna, Italy

Phase Images

SIR-C / Test Site: Mt. Etna, Italy

Mt. Etna

Interferometric SAR Implementations: Single vs. Repeat-Pass

Single-Pass or **Simultaneous Interferometry**

The two acquisitions are performed simultaneously

(Zero temporal baseline)

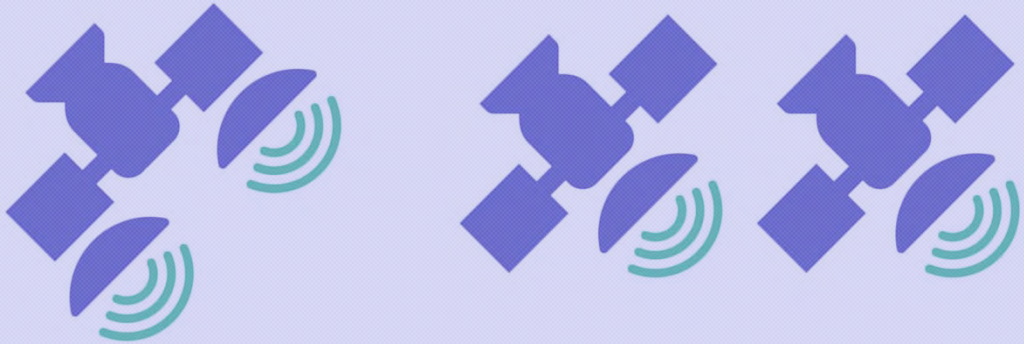

Single Platform
with two antennas

Two Platforms
flying in (close) formation

Repeat-Pass Interferometry

The two acquisitions are performed at different times

(Non-Zero temporal baseline)

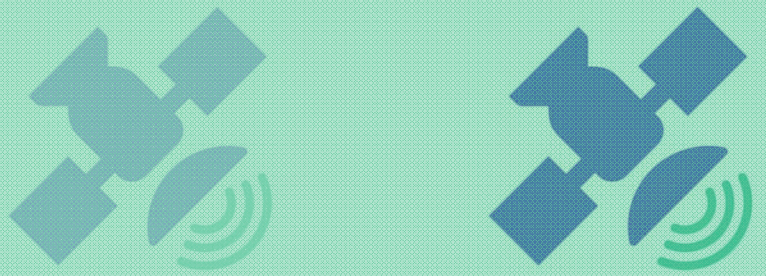

Single Platform
in repeated orbit(s)
or
Two Platforms
flying on the same orbit

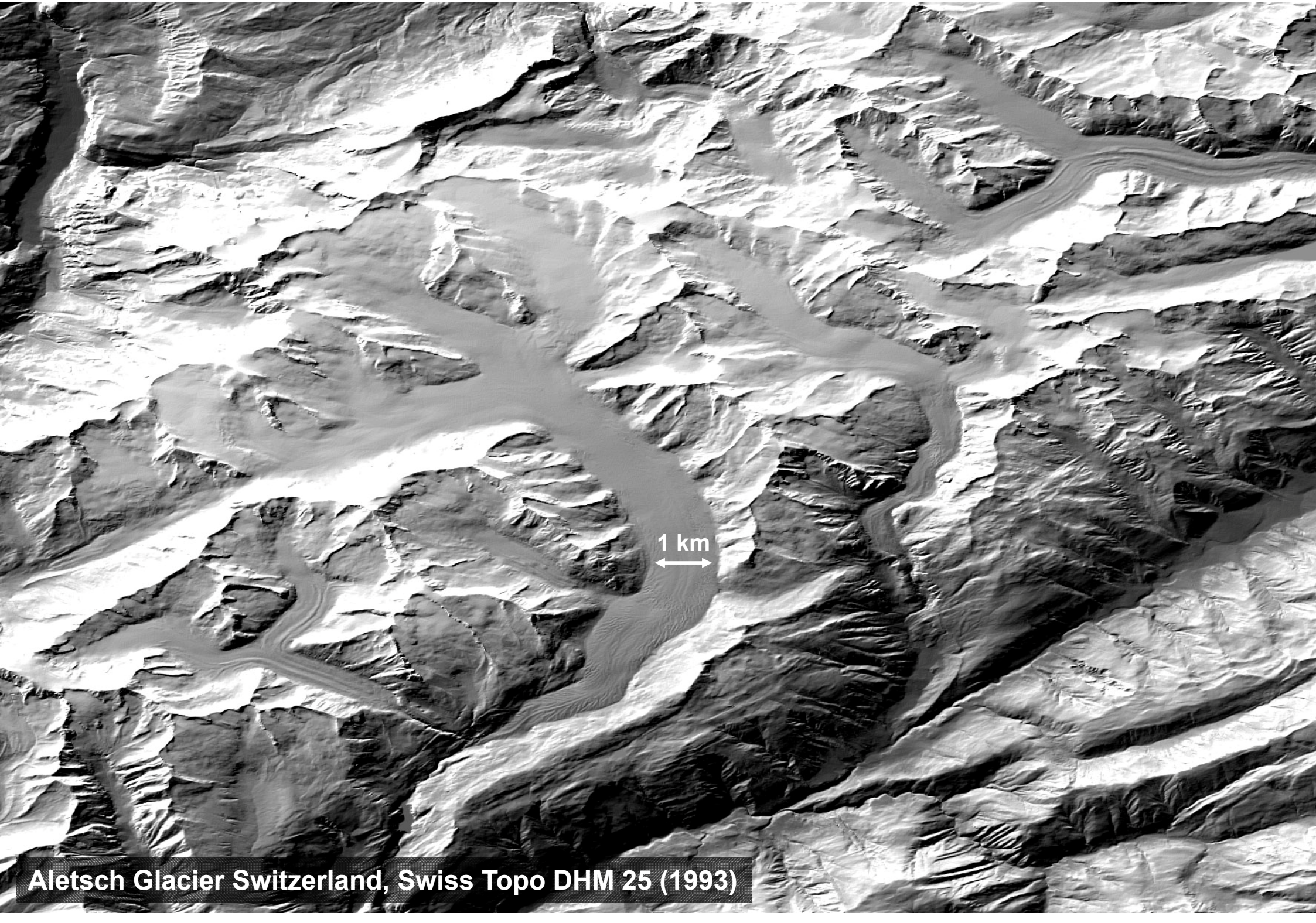

Aletsch Glacier Switzerland, Swiss Topo DHM 25 (1993)

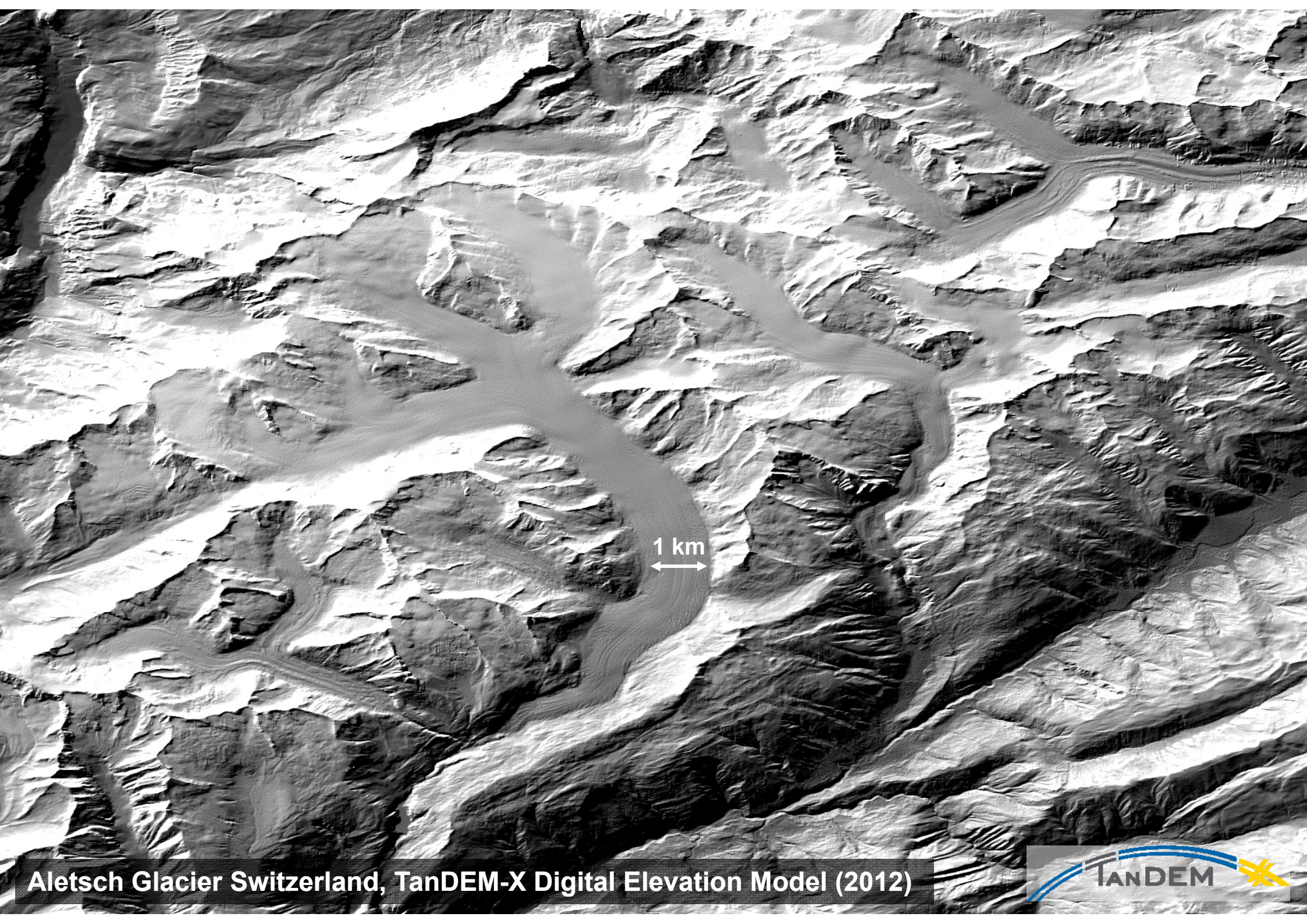
1 km
Aletsch Glacier Switzerland, TanDEM-X Digital Elevation Model (2012)
TanDEM

Snow Pack Monitoring by Means of DEM's

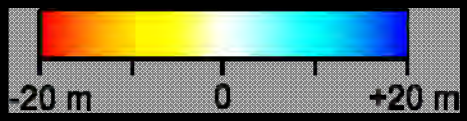

TanDEM-X vs. Alti3D (2011)

TanDEM

Aletsch Glacier: Annual/Seasonal Height Change

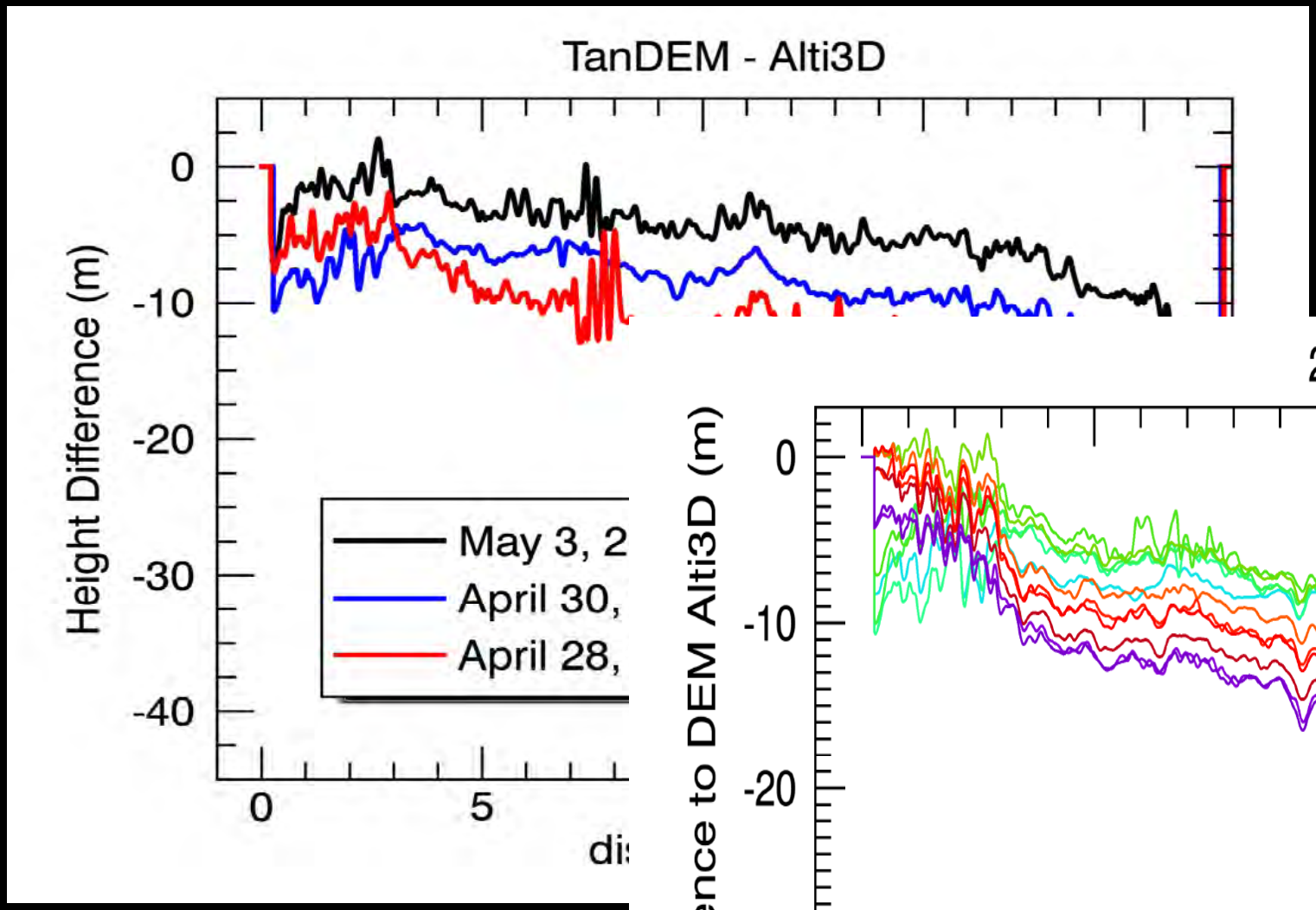

Annual

Height loss of 3-4 m/year

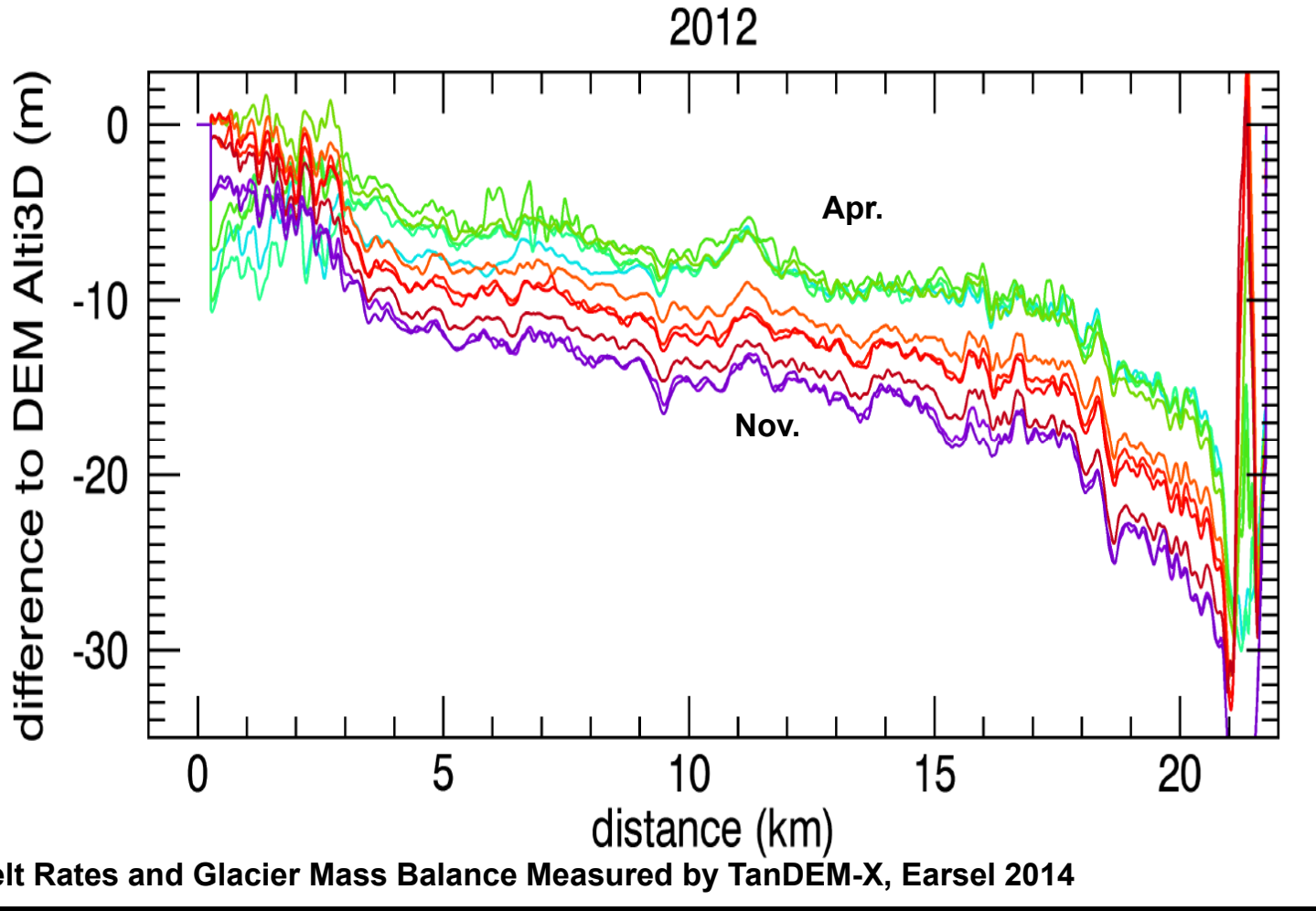

Seasonal

Leinss & Hajnsek, Snow Accumulation, Melt Rates and Glacier Mass Balance Measured by TanDEM-X, Earsel 2014

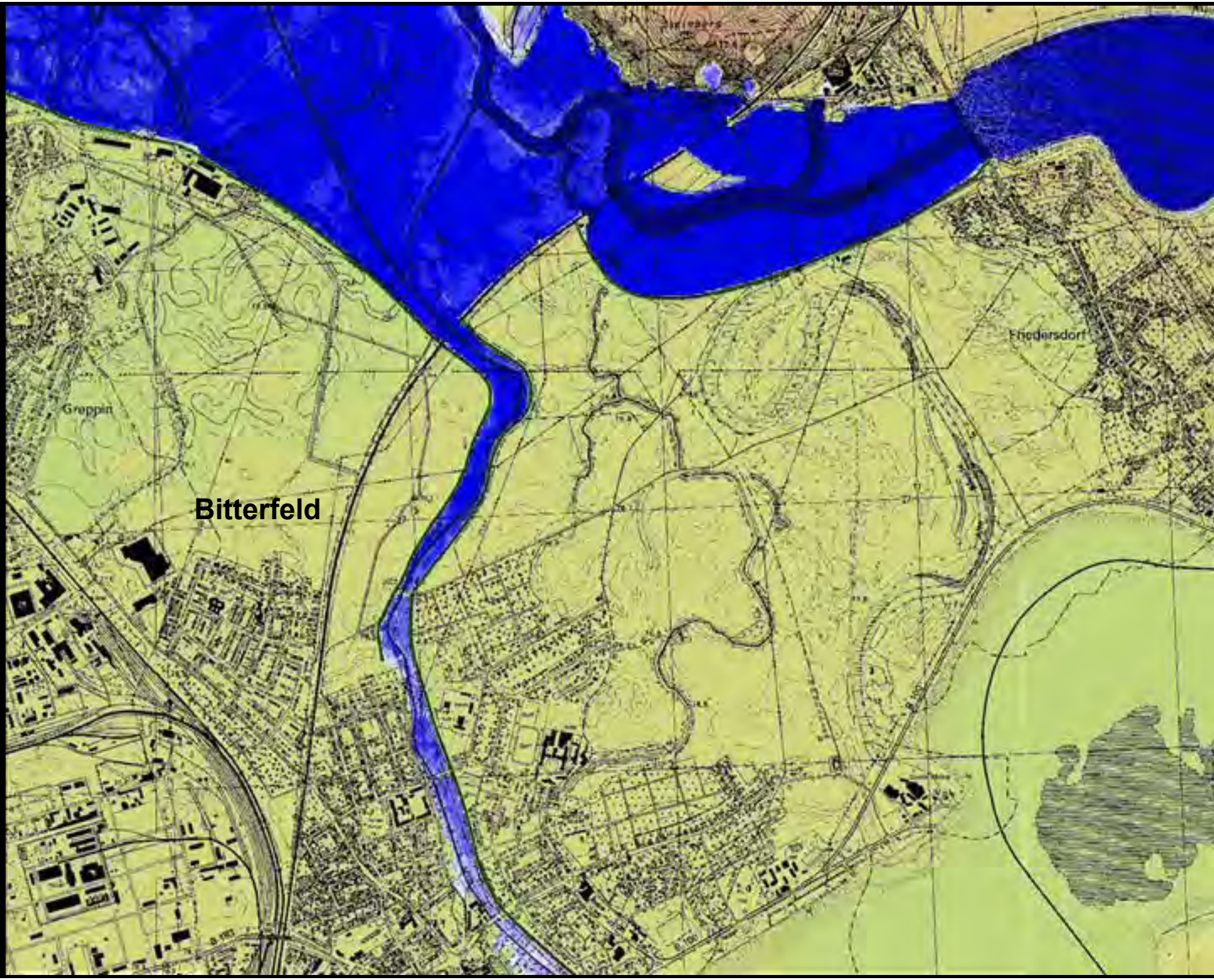
Greppin
Bitterfeld
Friedersdorf

Paddy Rice Monitoring by Means of DEM's

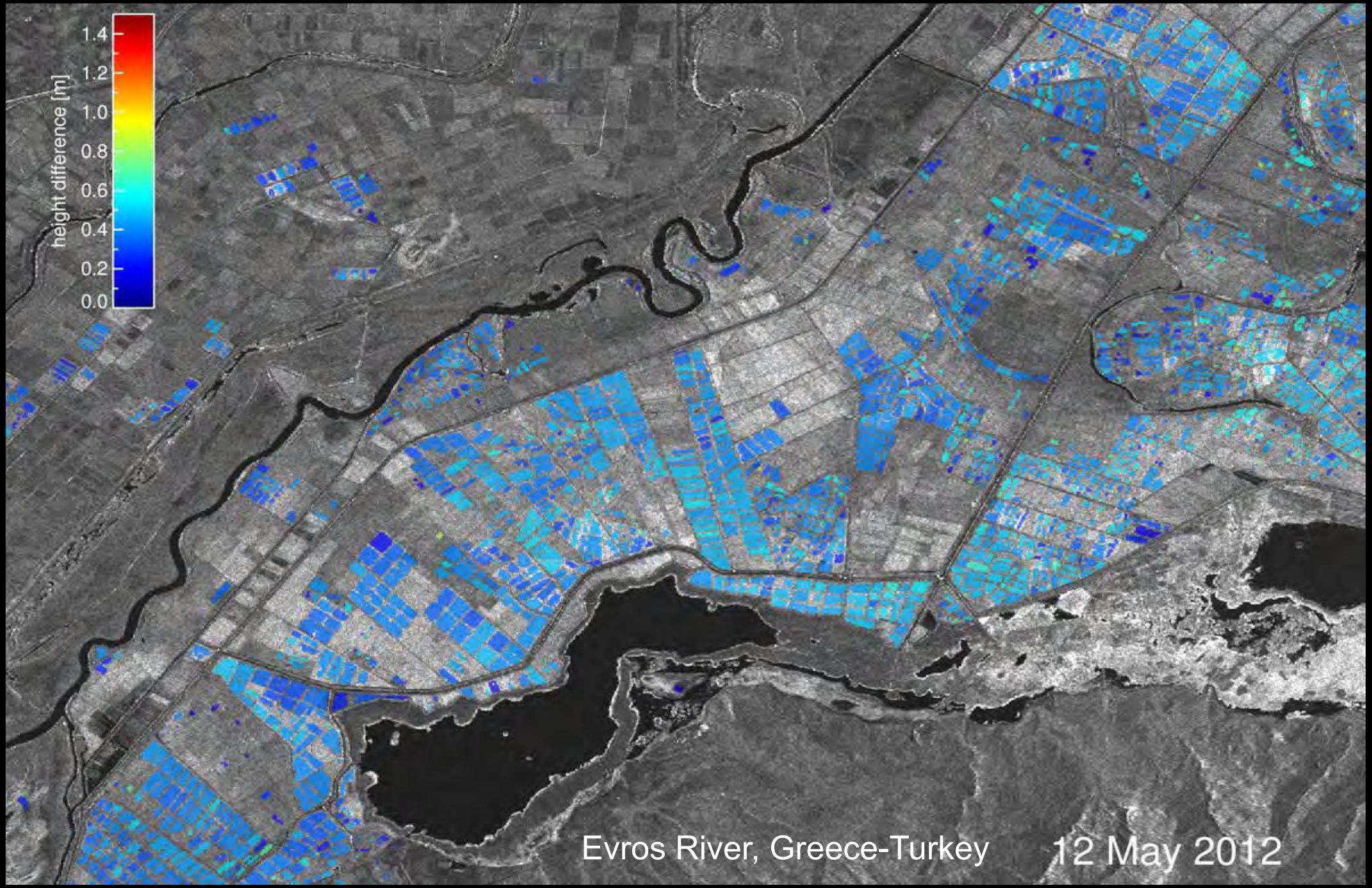

Paddy Rice Monitoring by Means of DEM's

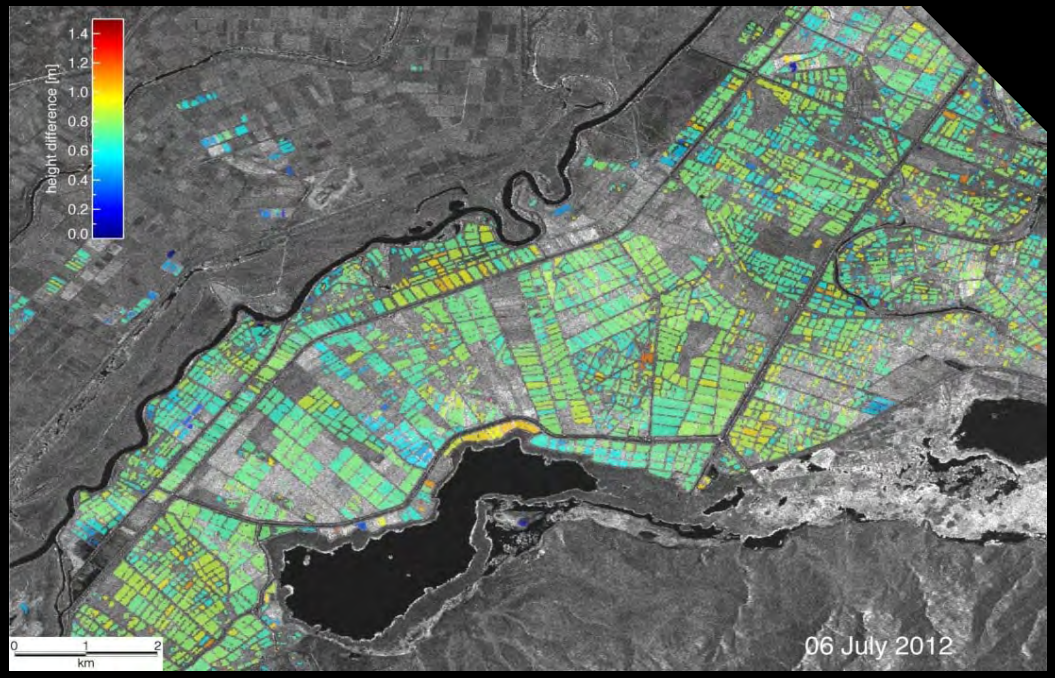

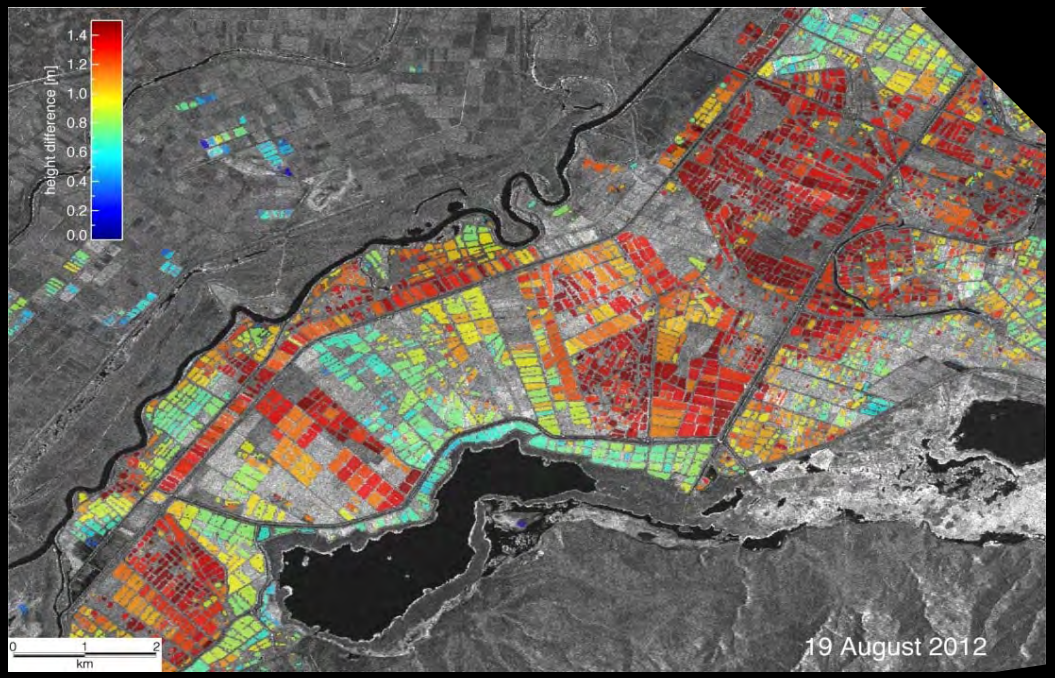

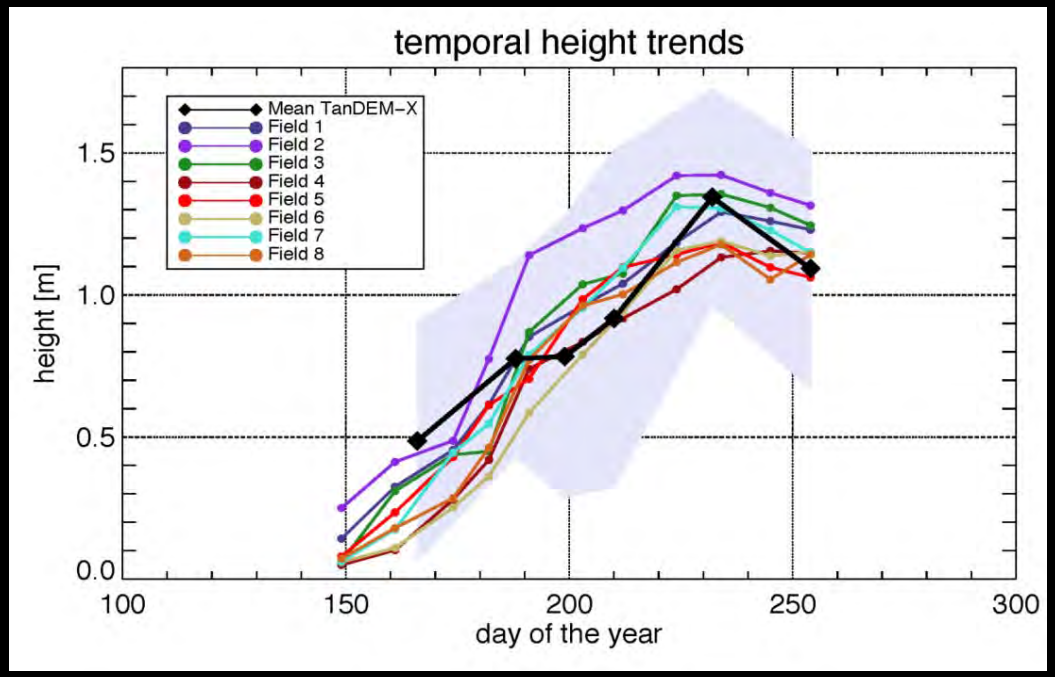

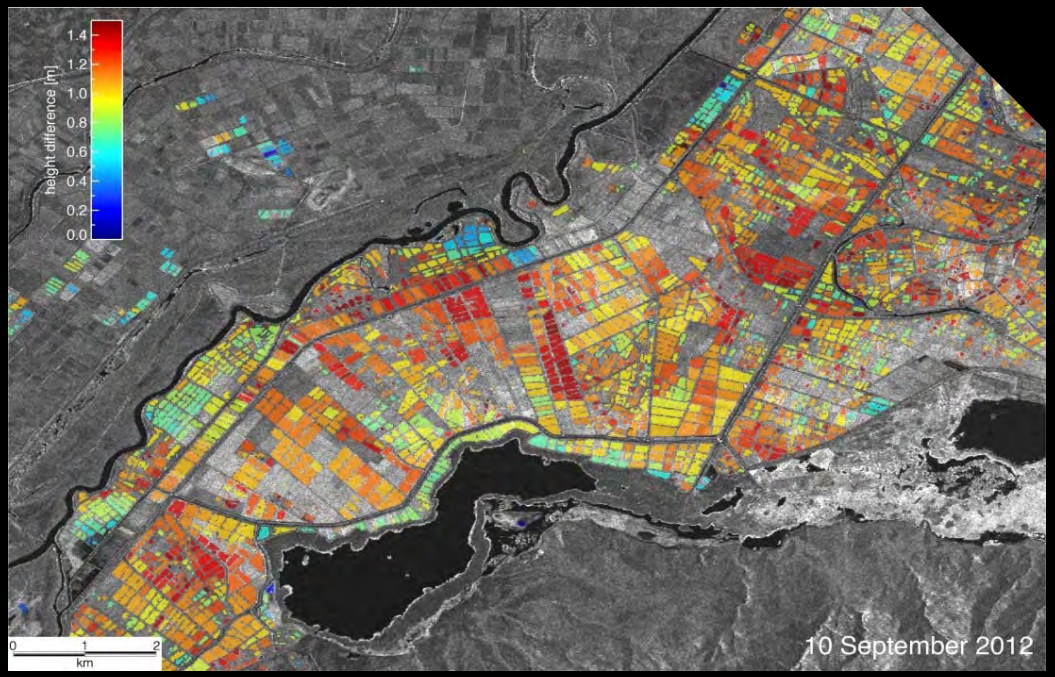

C. Rossi, and E. Erten, "Paddy rice monitoring using TanDEM-X", IEEE Transaction on Geoscience and Remote Sensing, 2015.

Differential SAR Interferometry

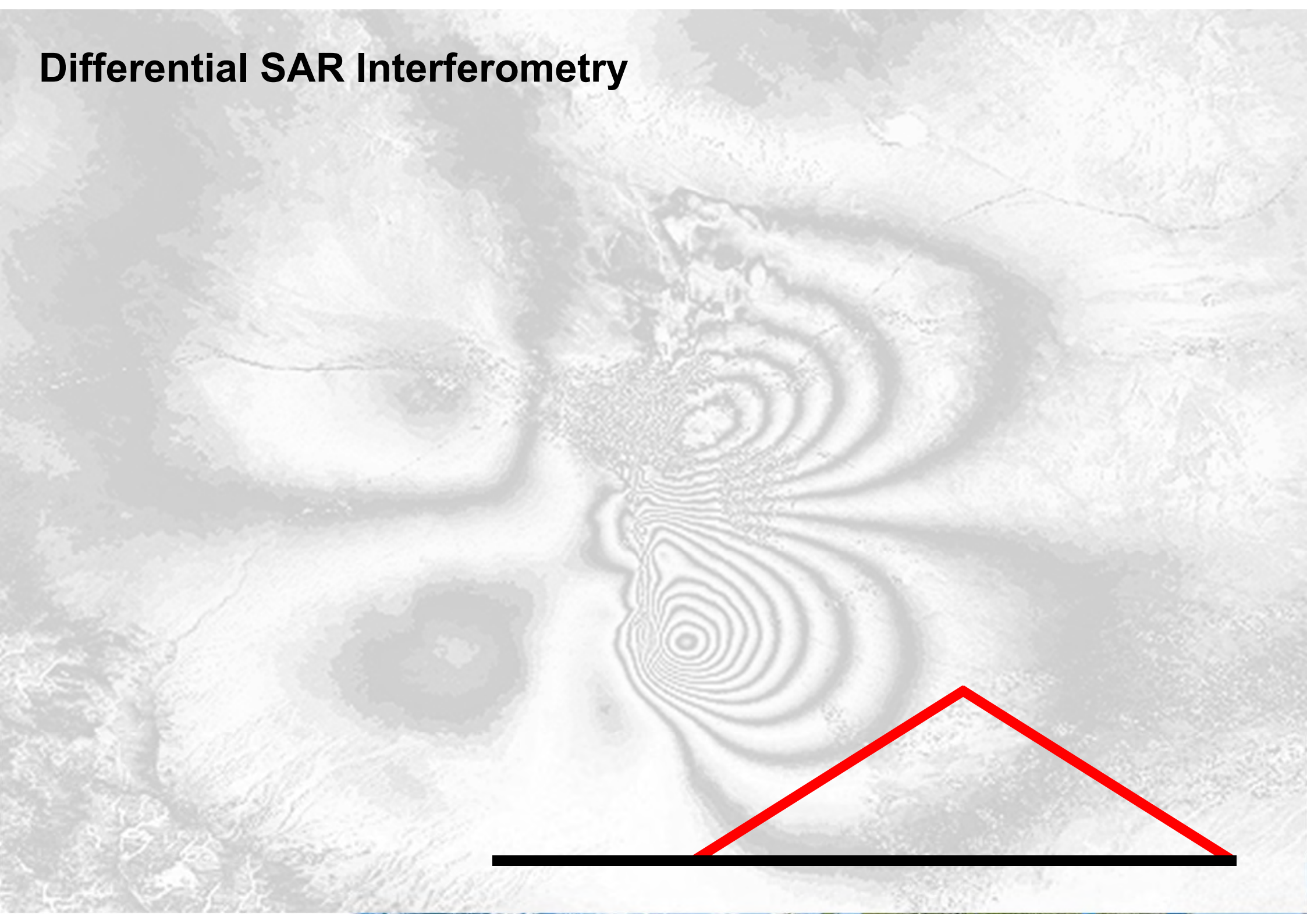

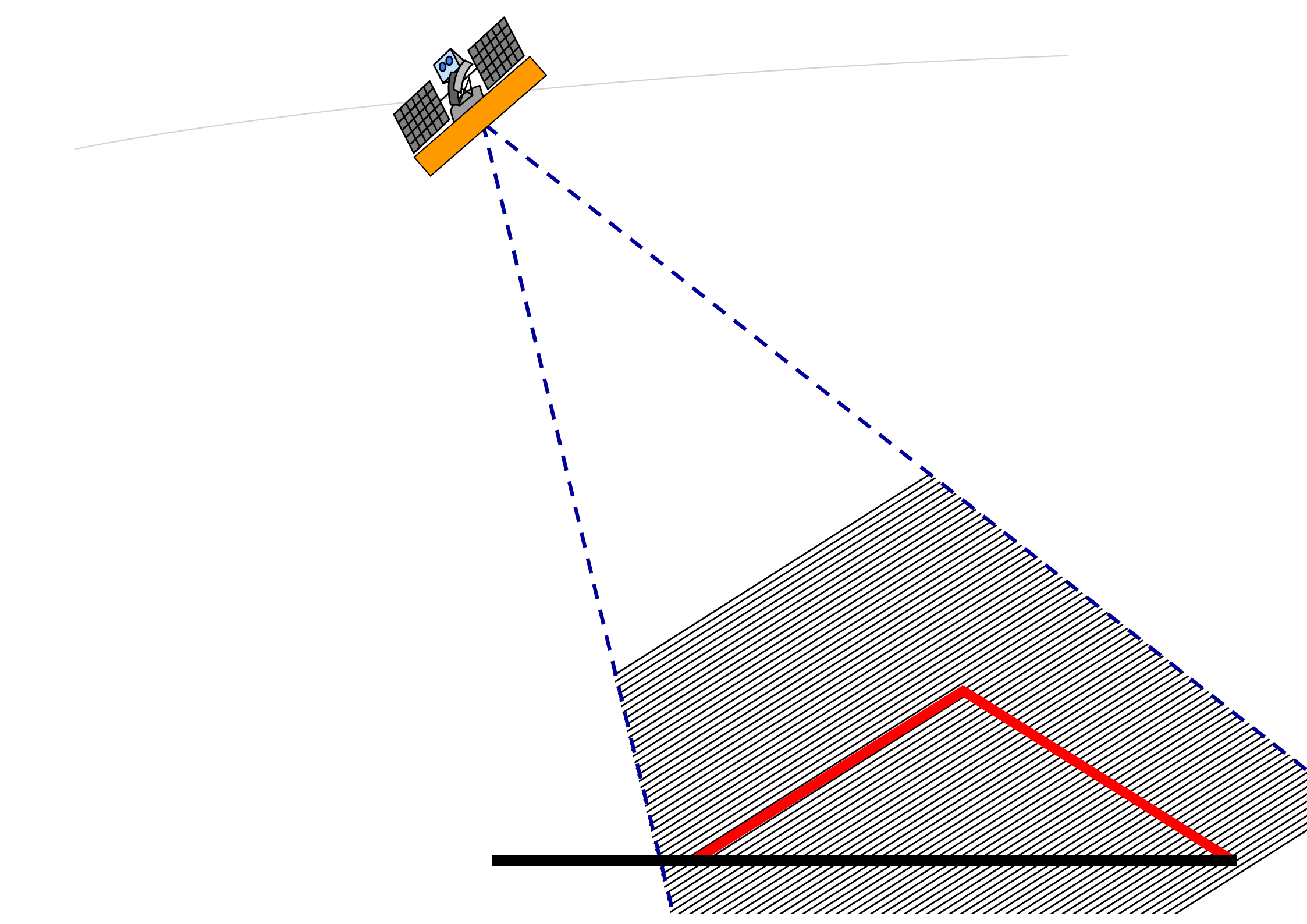

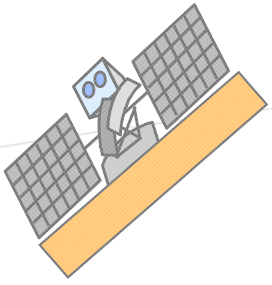

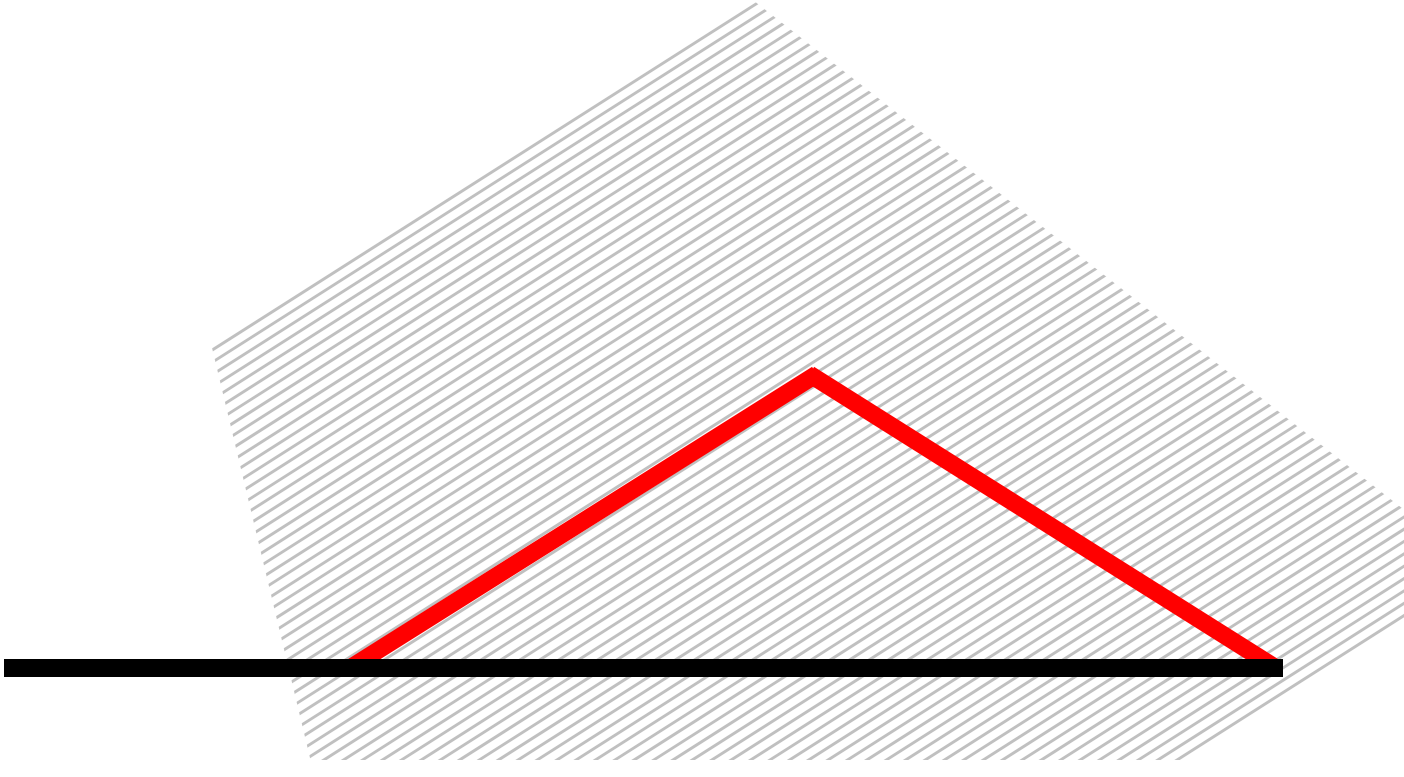

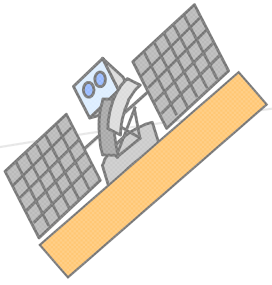

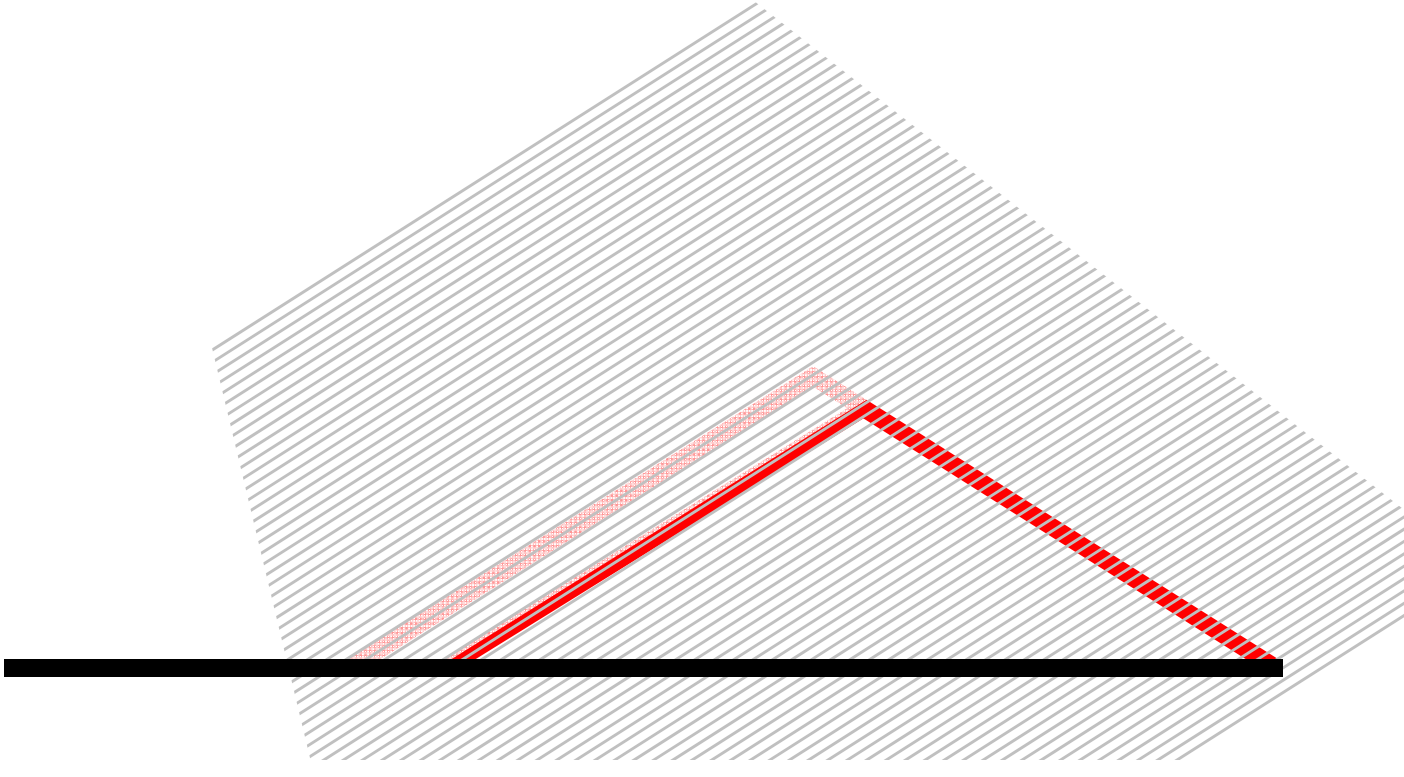

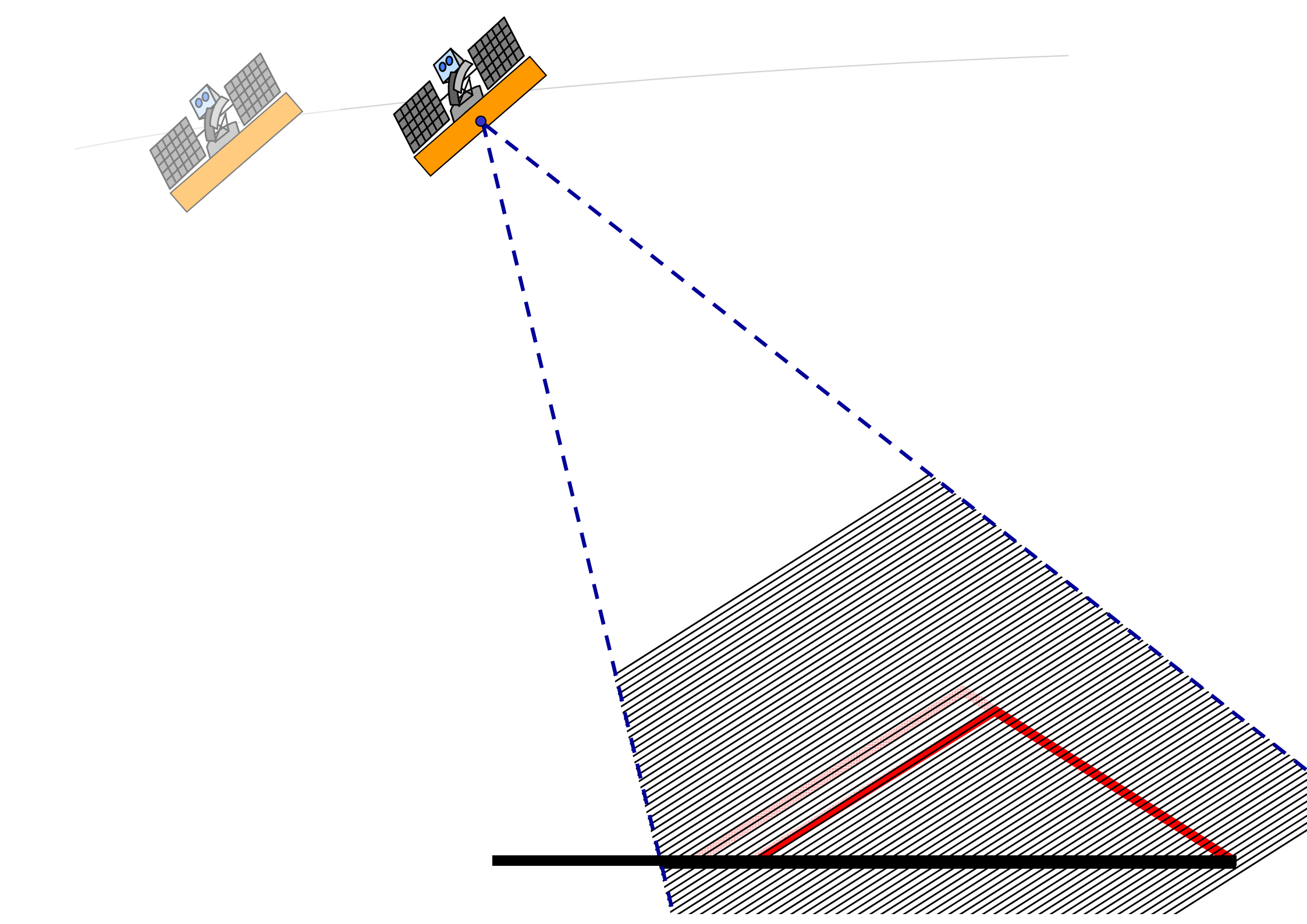

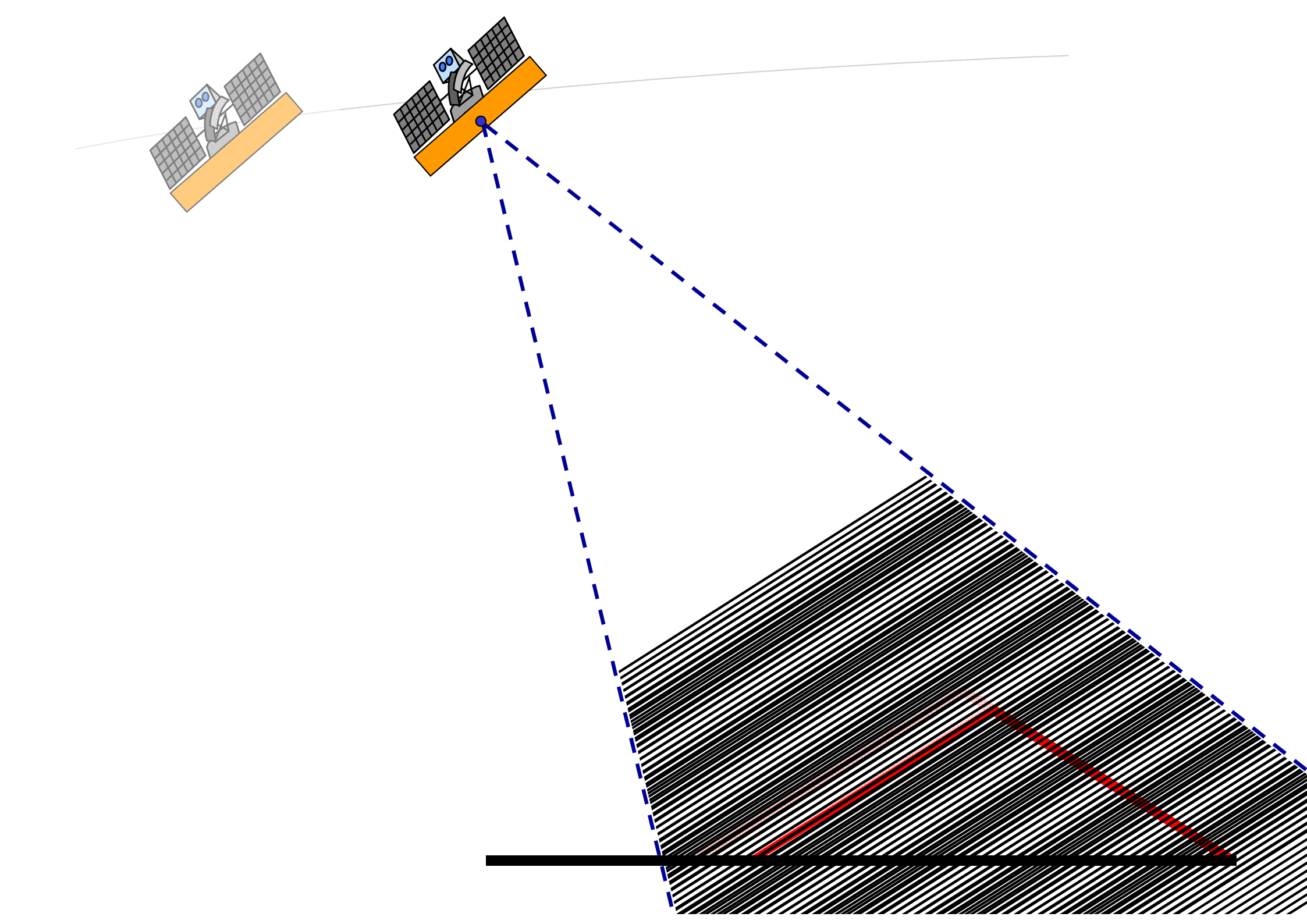

InSAR vs D-InSAR

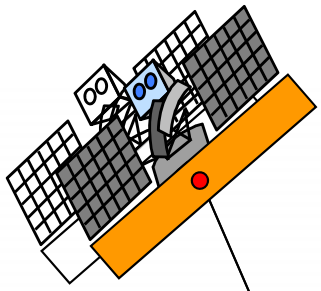

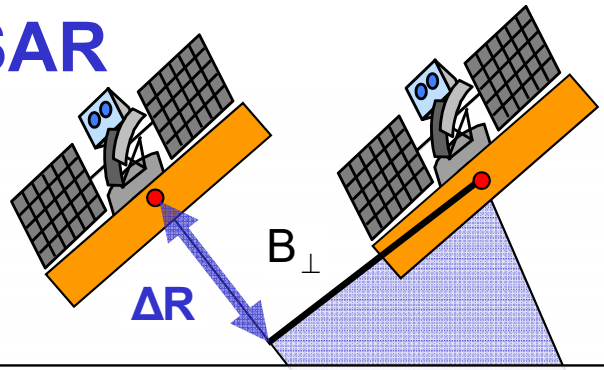

Example ERS: Space-borne C-band (Wavelength λ=0.056m) interferometer with incidence θ=23° at a range R=870Km. Assuming the ability to measure the interferometric phase with an accuracy of 20°:

D-InSAR

$$\sigma_R = \frac{\lambda}{4\pi}\sigma_\varphi = \frac{\lambda}{4\pi}\frac{20}{360}2\pi \approx 1.5 \text{ mm} \quad \text{(in LOS)}$$

$$\sigma_z = \frac{1}{\cos(\theta)}\sigma_R = 1.6 \text{ mm} \quad \text{(vertical)}$$

$$\sigma_y = \frac{1}{\sin(\theta)}\sigma_R = 4.0 \text{ mm} \quad \text{(horizontal)}$$

InSAR

$$\sigma_z = \frac{\lambda}{4\pi}\frac{R\sin(\theta)}{B_\perp}\sigma_\varphi = \frac{\lambda}{4\pi}\frac{R\sin(\theta)}{B_\perp}\frac{10}{360}2\pi$$

At perp. baseline $B_\perp$=100m: σ_z= 5.50m terrain error

At perp. baseline $B_\perp$=200m: σ_z= 2.75m terrain error

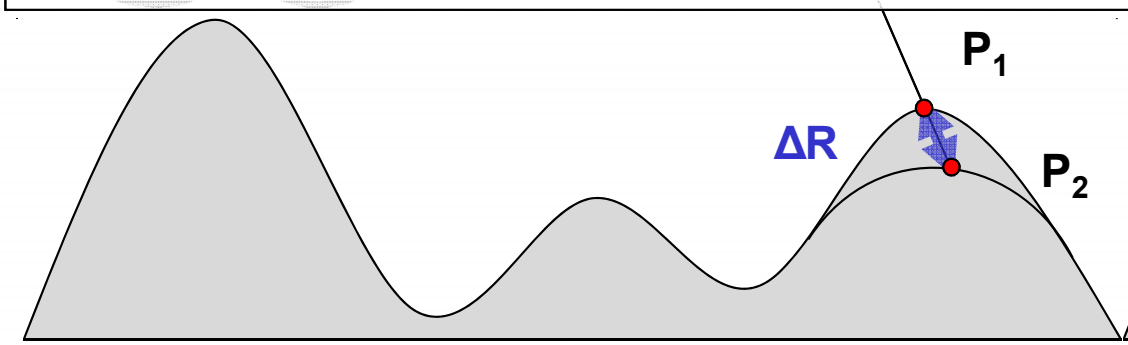

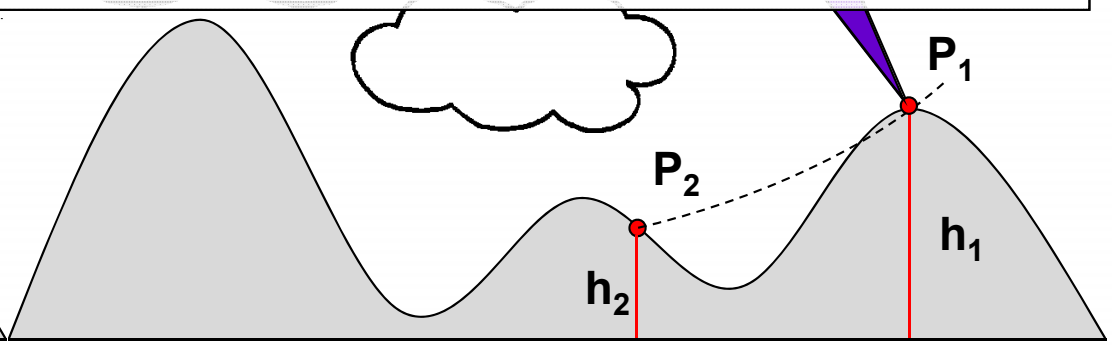

Seismic Faults: The Bam Earthquake by Envisat ASAR

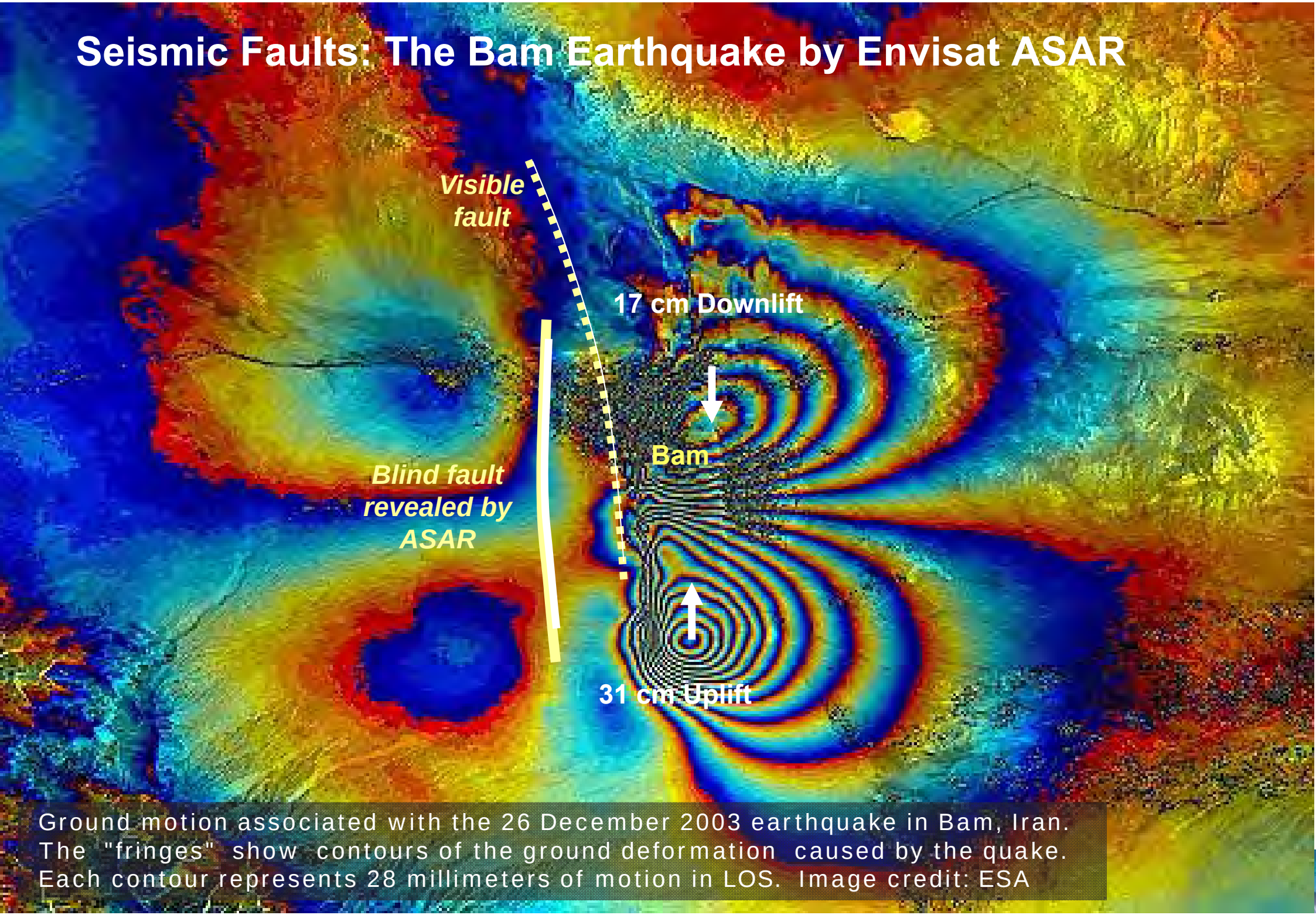

Ground motion associated with the 26 December 2003 earthquake in Bam, Iran. The "fringes" show contours of the ground deformation caused by the quake. Each contour represents 28 millimeters of motion in LOS. Image credit: ESA

Urban Subsidence

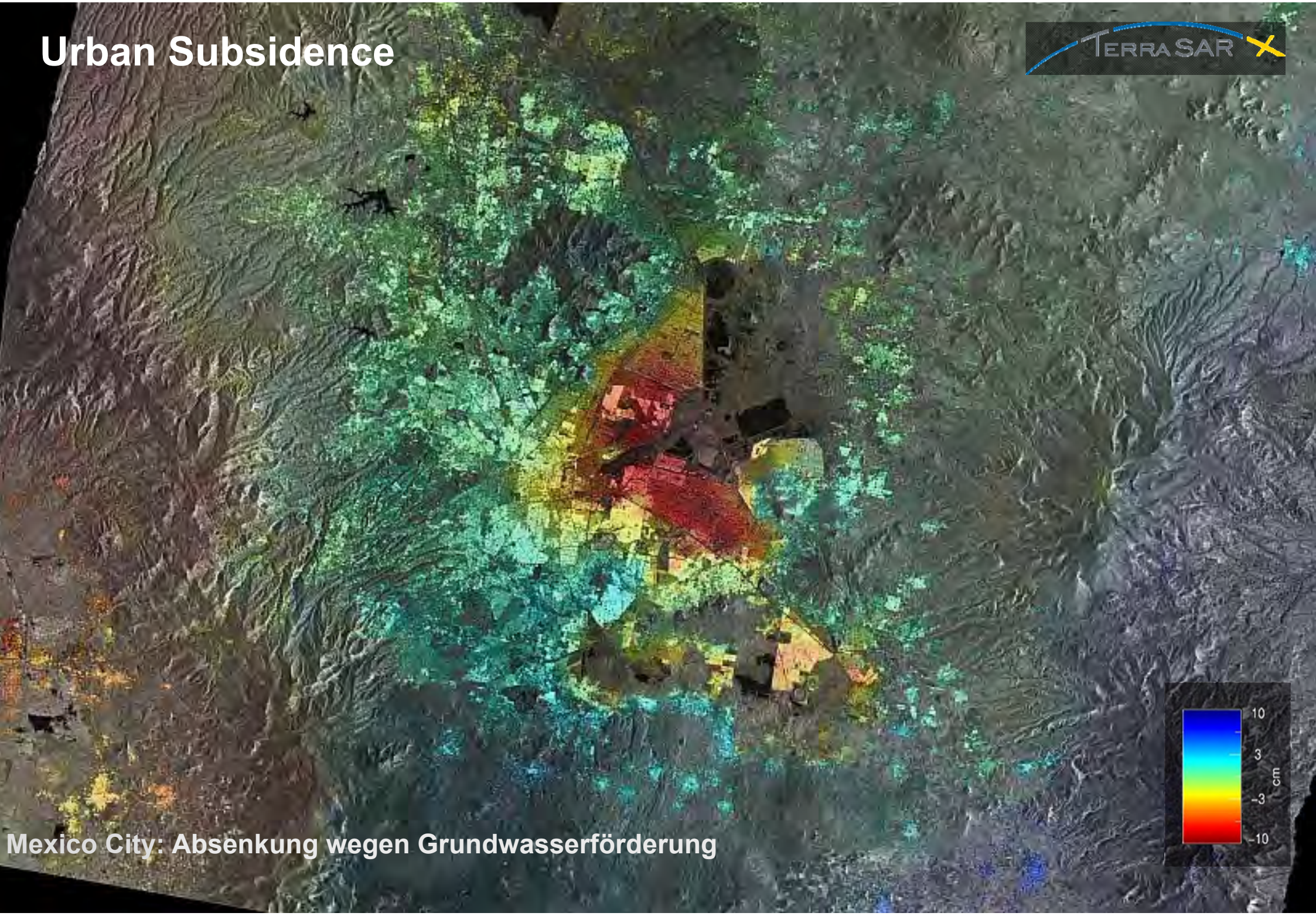

Mexico City: Absenkung wegen Grundwasserförderung

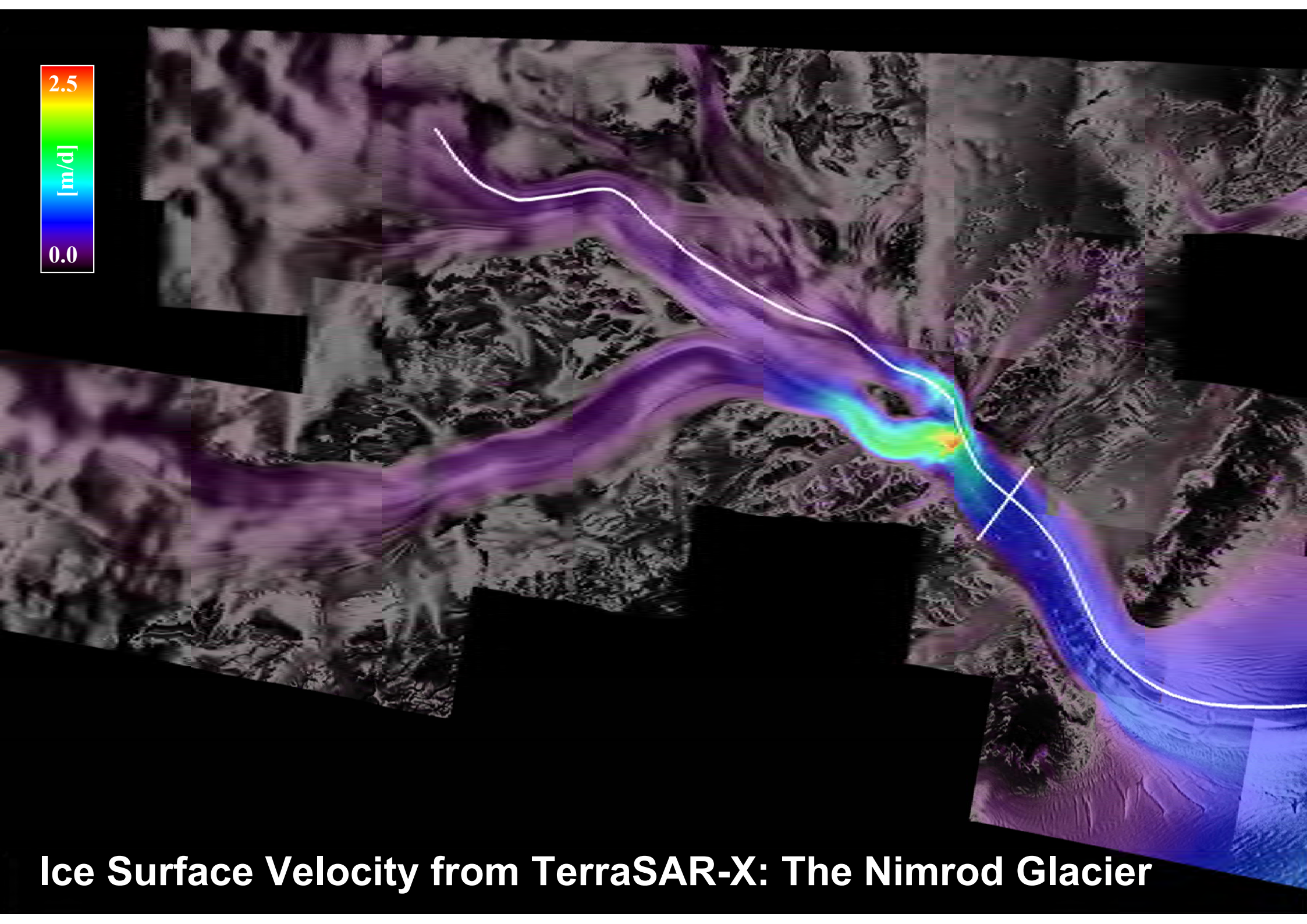

Ice Surface Velocity from TerraSAR-X: The Nimrod Glacier

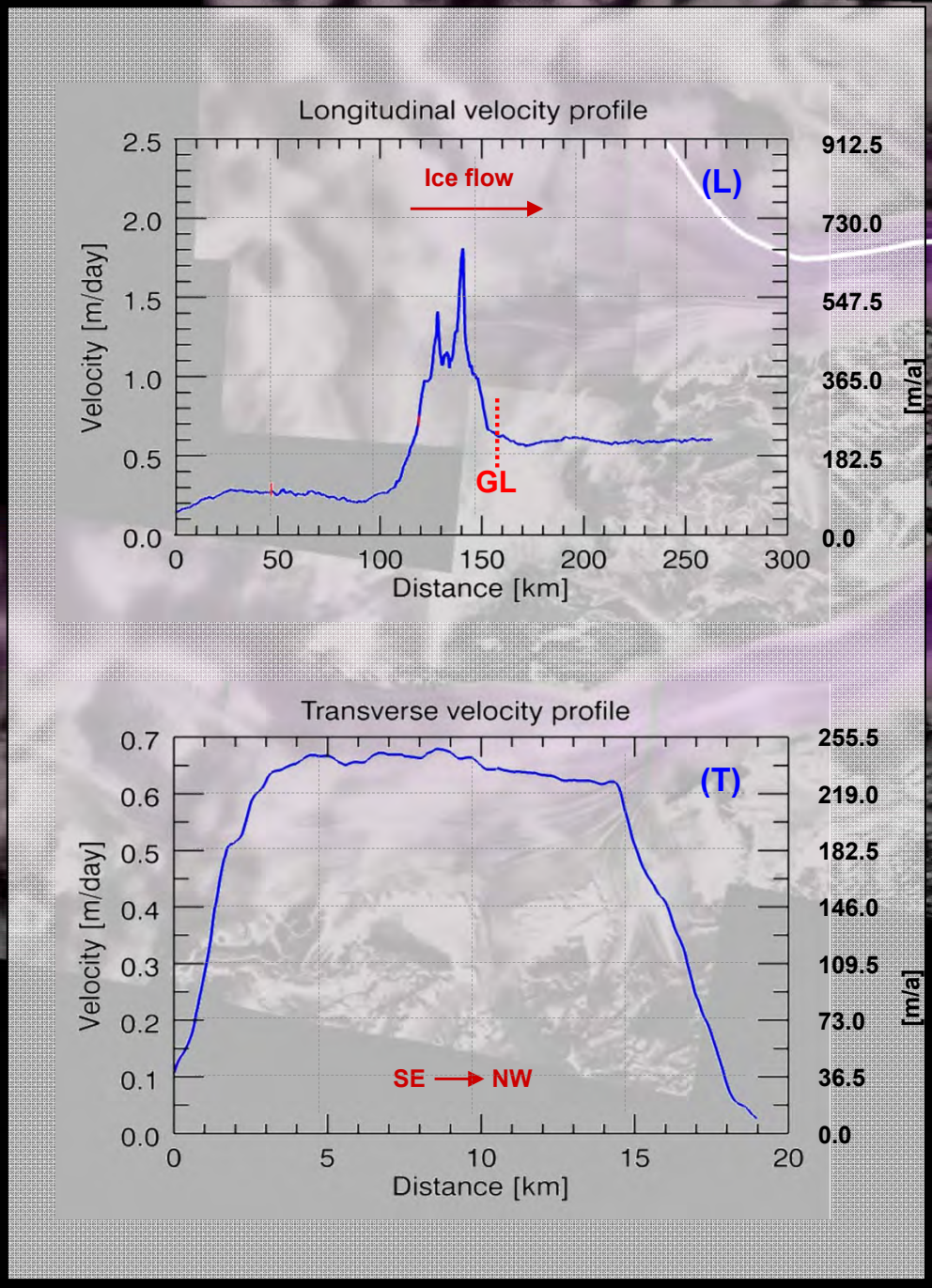

Ice Surface Velocity from TerraSAR-X: The Nimrod Glacier

Introduction to Synthetic Aperture Radar (SAR) and SAR-Interferometry (InSAR)

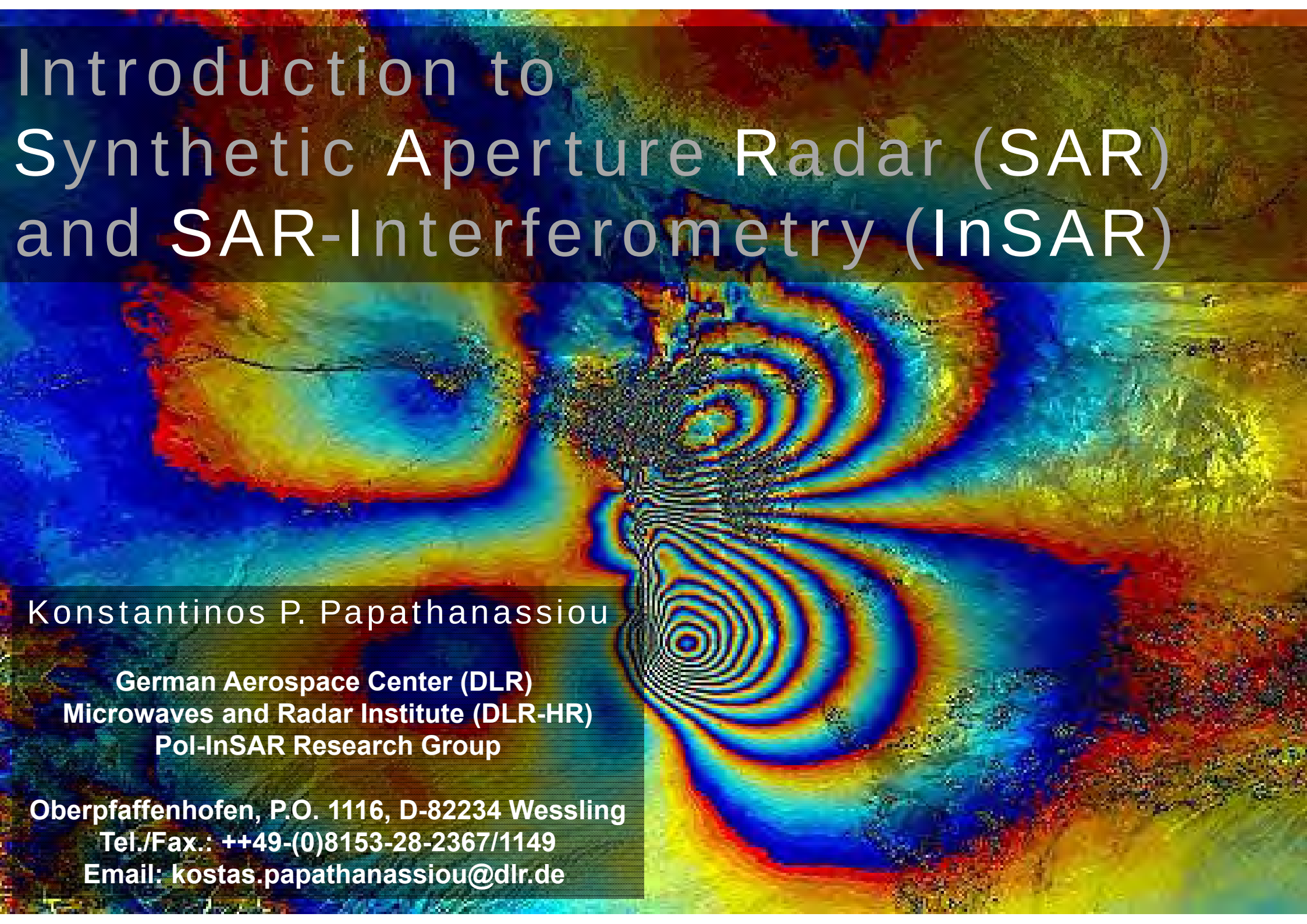

Konstantinos P. Papathanassiou

German Aerospace Center (DLR)
Microwaves and Radar Institute (DLR-HR)
Pol-InSAR Research Group

Oberpfaffenhofen, P.O. 1116, D-82234 Wessling
Tel./Fax.: ++49-(0)8153-28-2367/1149
Email: kostas.papathanassiou@dlr.de